Interactions of Novel Sets of Perylene Dianhydrides and a Diimide with G-Quadruplex Structures in Human DNA

Arwa Abou Rajab

Submitted to the
Institute of Graduate Studies and Research
in partial fulfillment of the requirements for the degree of

Master of Science
in
Chemistry

Eastern Mediterranean University
July 2018
Gazimağusa, North Cyprus

Approval of the Institute of Graduate Studies and Research

Assoc. Prof. Dr. Ali Hakan Ulusoy
Acting Director

I certify that this thesis satisfies all the requirements as a thesis for the degree of Master of Science in Chemistry.

Prof. Dr. İzzet Sakallı
Chair, Department of Chemistry

We certify that we have read this thesis and that in our opinion it is fully adequate in scope and quality as a thesis for the degree of Master of Science in Chemistry.

Assoc. Prof. Dr. Şükrü Tüzmen
Co-Supervisor

Prof. Dr. Huriye İcil
Supervisor

Examining Committee

1. Prof. Dr. Huriye İcil
2. Prof. Dr. Mehmet Özsöz
3. Prof. Dr. Şefik Süzer
4. Assoc. Prof. Dr. Şükrü Tüzmen
5. Asst. Prof. Dr. Rene M. Williams

ABSTRACT

Scientists from different fields have been coming together and trying to work on cancer therapies for many years. Recently, the interaction of perylene derivatives with G-quadruplex structures in human DNA has been studied for this purpose. Perylene derivatives have the ability to bind to the unusual DNA secondary structures called G-quadruplexes that form on specific regions of the human genome.

In this thesis, two perylene tetracarboxylic dianhydrides (PDA) and a perylene diimide (PDI) were observed with regard to their interactions with G-quadruplex DNA. A PCR (polymerase chain reaction) amplified region from the human beta globin gene was used to prove the formation of G-quadruplex structures in the presence of repetitive guanine bases, and c-kit and a-coreTT were used as the guanine rich oligonucleotides. The complexations were analyzed using absorption and emission spectroscopy and gel electrophoresis techniques.

Absorption and emission investigations have illustrated a variation in the peaks of the primers and compounds when the complexation was performed. Electrophoresis results have shown that bands with the PCR product alone migrate faster than the bands with the PCR product and the perylene derivative together. Overall, the investigated perylene derivatives have a potential binding affinity towards G-quadruplex structures throughout the human genome.

Keywords: Perylene derivatives, G-quadruplex, cancer therapy, beta globin gene, telomeric region, promoter region.

ÖZ

Farklı alanlardan bilim adamları uzun yıllardır bir araya gelip kanser tedavileri üzerinde çalışmaktadır. Kanser tedavisi amacı ile, son zamanlarda perilen türevlerinin insan DNA'sındaki G-quadruplex yapılarıyla etkileşimi incelenmiştir. Perilen türevleri insan DNA'sının belirli bölgelerinde oluşan G-quadruplex adı verilen olağandışı DNA sekonder yapılarına bağlanma yeteneğine sahiptir.

Bu tezde, iki perilen tetrakarboksilik dianhidrit ve bir perilen diimid türevinin insan DNA'sındaki G-quadruplex yapıları ile etkileşimi gözlemlenmiştir. Polimeraz zincir reaksiyonu ile insan beta globin geninden amplifiye edilmiş bir bölge, G-quadruplex yapılarının ard arda tekrarlayan guanin bazlarının varlığıyla oluştuğunu ıspatlamak amacıyla kullanılmıştır. Guanin bazı ile zengin oligonükleotidler olarak da c-kit ve a-coreTT kullanılmıştır. Kompleksleşme, absorpsiyon ve emisyon spektroskopisi ile jel elektroforezi teknikleri kullanılarak analiz edilmiştir.

Absorpsiyon ve emisyon incelemeleri, kompleksleştirmenin sadece primerler ve bileşiklere ait absorpsiyon ve emisyon piklerinde bir varyasyona neden olduğunu göstermektedir. Elektroforez sonuçları, sadece polimeraz zincir reaksiyonu ürünü içeren bantların polimeraz zincir reaksiyonu ürünü ve perilen türevini birlikte içeren bantlardan daha hızlı koştuğunu göstermiştir. Sonuç olarak incelenen perilen türevleri, insan genomunda bulunan G-quadruplex yapılarına karşı potansiyel bir bağlanma afinitesine sahiptir.

Anahtar Kelimeler: Perilen türevleri, G-quadruplex, kanser tedavileri, beta globin geni, telomerik bölge, promoter bölge.

To My Family

(Every Success Story Started With a Dream!)

ACKNOWLEDGEMENT

I would like to appreciate the opportunity that was given to me by my supervisor Prof. Dr. Huriye İcil to be working on both my undergraduate field, Molecular Biology and Genetics, and Organic Chemistry together to end up with an interesting topic. I would like to thank her for her huge motivation, support, understanding and kindness. I would also like to express my sincere appreciation to my co-supervisor Assoc. Prof. Dr. Şükrü Tüzmen for his contribution, precious advices and guidance that resulted with a positive outcome for me.

I would like to thank Dr. Duygu Uzun for being always there for me whenever I needed any help, and also for her valuable advices and motivation.

Special thanks go to my precious parents Rana Allouch and Assist. Prof. Dr. Hassan Abou Rajab that always stood by me and were proud of me at every step of my life. The support and motivation of my siblings and my friends was also very special for me.

TABLE OF CONTENTS

LIST OF TABLES

LIST OF FIGURES

LIST OF SYMBOLS AND ABBREVIATIONS

bp	Base Pairs
℃	Degree Celsius
DNA	Deoxyribonucleic Acid
dNTPs	2'-deoxynucleoside 5'-triphosphates
DSSCs	Dye-Sensitized Solar Cells
Eqn	Equation
FT-IR	Fourier Transform Infrared Spectroscopy
G4	G-quadruplex
G-rich	Guanine Rich
G-tetrad	Guanine Tetrad
h	Hour
hTERT	Human Telomerase Reverse Transcriptase
M	Molarity
m	Mass
mL	Milliliter
M_w	Molecular Weight
µg	Microgram
µL	Microliter
µM	Micromolar
nm	Nanometers
NMR	Nuclear Magnetic Resonance
PCR	Polymerase Chain Reaction
PDA	Perylene-3,4,9,10-tetracarboxylic dianhydride

PDI	Perylene Diimide
pmol	Picomol
TAE	Tris-acetate-EDTA
T_m	Primer Melting Temperature
u	Unit
UV-vis	Ultraviolet, Visible Light Absorption
V	Volt
V	Volume
VEGF	Vascular Endothelial Growth Factor
λ_{exc}	Excitation Wavelength
λ_{max}	Wavelength Where Absorbance is Maximum

Chapter 1

INTRODUCTION

Perylene dyes have a wide range of applications, ranging from dye-sensitized solar cells (DSSCs) [1] and electron transfer studies [2] to biomedical applications [3]. Their studies are getting more and more interesting for the huge area of science due to their potential to act as transcriptional regulators [4], anti-angiogenesis agents [5], telomerase inhibitors [6] and antineoplastic agents [7]. The potential of perylene analogues to have a role in cancer therapy has been studied before and is still a topic of interest today [8, 9].

The richness of promoter regions of oncogenes in guanine bases is a potential for the formation of the secondary structures called G-quadruplexes (G4). Evidence that two G4 forming sequences exist in both the promoter regions of the c-myc and c-kit genes was previously found by Nuclear Magnetic Resonance (NMR) spectroscopy [10] and the transcription of those genes was silenced by organic molecules [11, 12]. Similarly, the G4 structures formed in human telomeres were efficiently studied before by the aid of spectroscopic measurements as well as X-ray diffraction [13].

In 2012, Taka et al. studied several perylene derivatives for their potential application as anti-angiogenesis agents and they illustrated that among the molecules that were investigated, a perylene derivative was capable of decreasing the activity of the Vascular Endothelial Growth Factor (VEGF) gene [5]. In 2013, Taka's group

studied their perylene derivatives again but this time with regard to their ability to induce the formation of G4 structures at the single strand overhang of the human Telomerase Reverse Transcriptase (hTERT) promoter as well as the human telomeres. They have found that both of the perylene derivatives are able to decrease both the expression of hTERT and the activity of telomerase, suggesting that telomerase inhibition is another promising therapy for cancer [14].

Moreover, Sissi et al. studied some perylene derivatives for their deoxyribonucleic acid (DNA) telomerase inhibition property and they concluded that further investigation could result in antineoplastic agents based on the perylene analogues that they investigated. The point behind this mechanism is the role of guanine rich (G-rich) tandem repeat in the human telomeres [7].

Following Taka's group, in 2014, Xu et al. continued to work on perylenes and they have synthesized a unique perylene-based DNA intercalator with a positively charged polar side chain that would increase the solubility of the dye. By this way the dye will be able to enter into the cell nuclei and then therefore intercalate into DNA. There is an emphasis that dyes used for those purposes require water solubility and high fluorescence quantum yield in water due to the necessity of further investigation in cell lines. Absorption and emission spectroscopy have been used to study the binding interaction between the perylene dye and the DNA [9].

Rossetti's group found that the inhibition of telomerase by perylene derivatives is dependent on both the length and the basicity of the side chains. This group has shown that the inhibition of telomerase by perylene derivatives with too short and/or a weakly basic side chain was poor [15]. In another study by Kerwin et al, the

binding selectivity of the perylene derivatives toward duplex and quadruplex DNA was investigated with regard to self-mediated aggregation, suggesting that extensive aggregation of perylene dyes causes preferential binding to G4 DNA over duplex DNA. This means that the perylene derivatives will not bind anywhere on the human genome, but rather on the regions of the genome that have formed a G4 structure [16].

The aim of this study was to investigate the binding interaction of three different perylene derivatives; N,N'-bis(4-benzosulfonic acid)perylene-3,4,9,10-tetracarboxylic diimide (SPDI), 1,7-di(3,5-diamino-pyrimidoxyl)perylene-3,4,9,10-tetracarboxylic dianhydride (YPDA) and 1,7-di(thiazolium)perylene-3,4,9,10-tetracarboxylic dianhydride (CPDA) provided in Figure 1.1 with the guanine rich (G-rich) oligonucleotides provided in Table 1.1. The two primers, PCO3 and CD6, were used to amplify a guanine rich region from the human beta globin gene (exon I, exon II and 60 base pairs (bp) of intron II after exon II) using PCR [17, 18]. Their aim was to prove the principle that repetitive guanine rich regions throughout the human genome are able to fold into G-quadruplex structures. This step was investigated via gel electrophoresis. G-rich oligonucleotides from the human telomeres (a-coreTT) [19] and promoter region (c-kit) were also used [19] for the interaction with the three perylene derivatives. Absorption and emission spectroscopy techniques were used for this investigation. The main purpose of this study was to observe if guanine rich regions throughout the human genome have a potential to form a G4 structure in the presence of perylene dyes. Short oligonucleotides from the human telomeres and a promoter region as well as a 595 bp region from the human beta globin gene were used for the investigation.

Table 1.1: The Oligonucleotides and Their Sequences

Oligo Name	Sequence (5'-3')
a-coreTT	AGGGTTAGGGTTAGGGTTAGGGTT
c-kit	AGGGAGGGCGCTGGGAGGAGGAGGG
PCO3(F)	ACACAACTGTGTTCACTAGC
CD6(R)	ATTCGTCTGTTTCCCATTCTAAAC

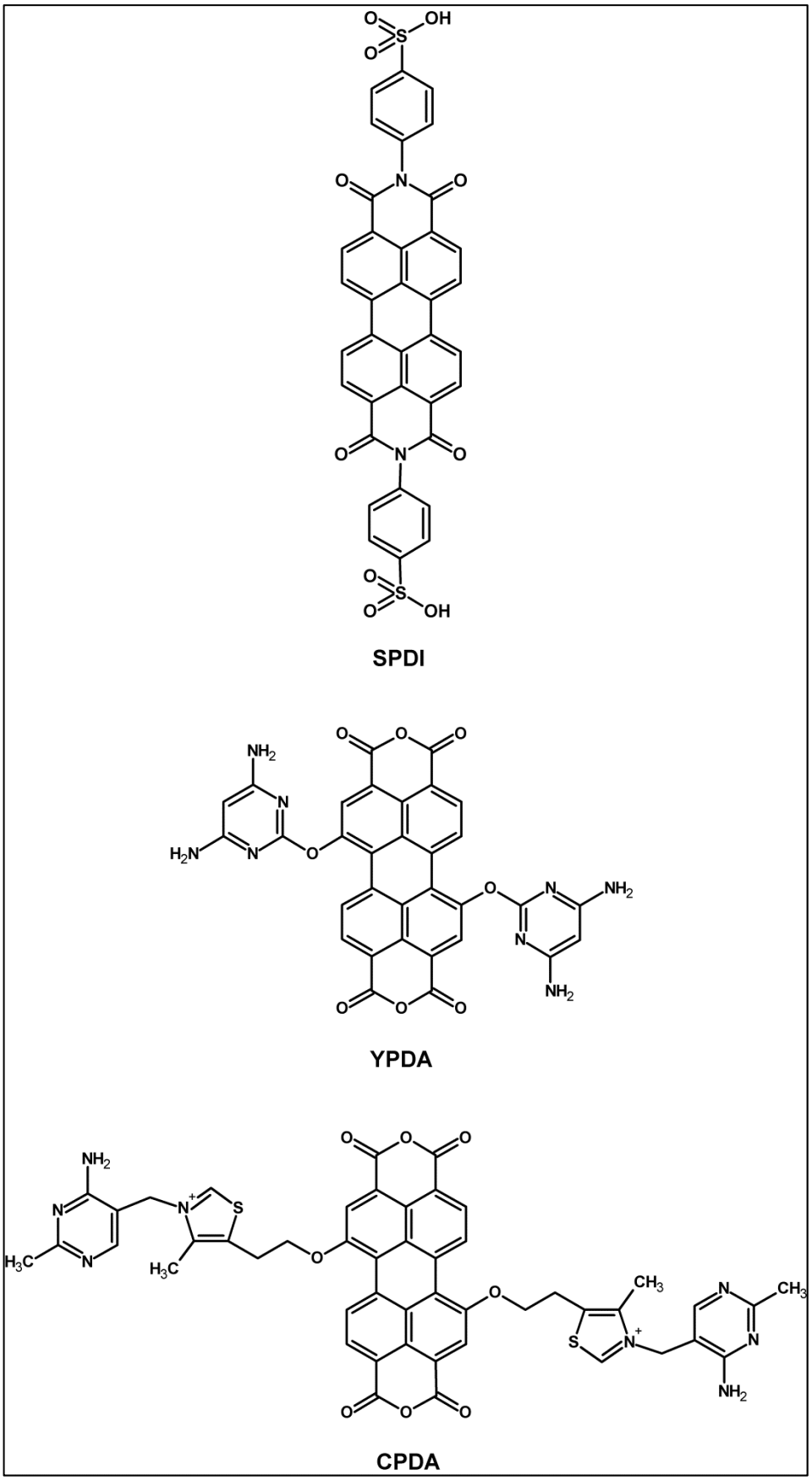

Figure 1.1: Chemical Structures of SPDI, YPDA and CPDA

Chapter 2

THEORETICAL

2.1 Different DNA Architectures - G-Quadruplex Structures

Characterization of DNA, the key for genetic material, by Watson and Crick in 1953 has been one of the most challenging discoveries of all times. They have demonstrated that the DNA double helix is made up of adenine bases hydrogen bonded to thymine bases and guanine bases hydrogen bonded to cytosine bases [20, 21]. Figure 2.1 illustrates a detailed structure of DNA [22] and Figure 2.2 shows the Watson-Crick base pairing [23]. Additionally, DNA could actually take up various conformations other than the right-handed double helical structure of B-DNA that was acknowledged in 1953. Higher order structures of DNA were first identified by Bang in 1910 and he suggested that guanine rich regions of the genome are the key point for this kind of structures [24].

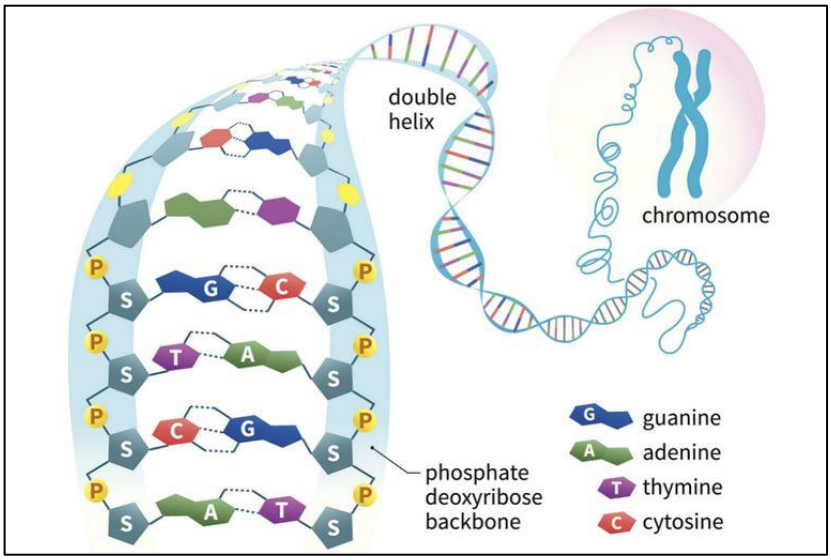

Figure 2.1: Detailed Structure of a DNA Double Helix

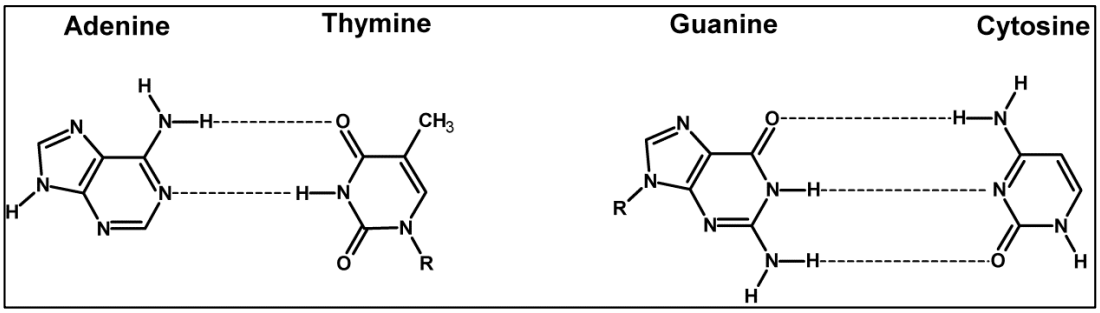

Figure 2.2: Watson-Crick Base Pairing

In 1962, tetrameric structures of DNA were observed by Gellert and his colleagues by the aid of X-ray diffraction. Guanine bases have a capacity to form Hoogsteen hydrogen bonding which is different than the Watson–Crick base pairing in the DNA double helix. Figure 2.3 shows the bonding sides of a guanine base.

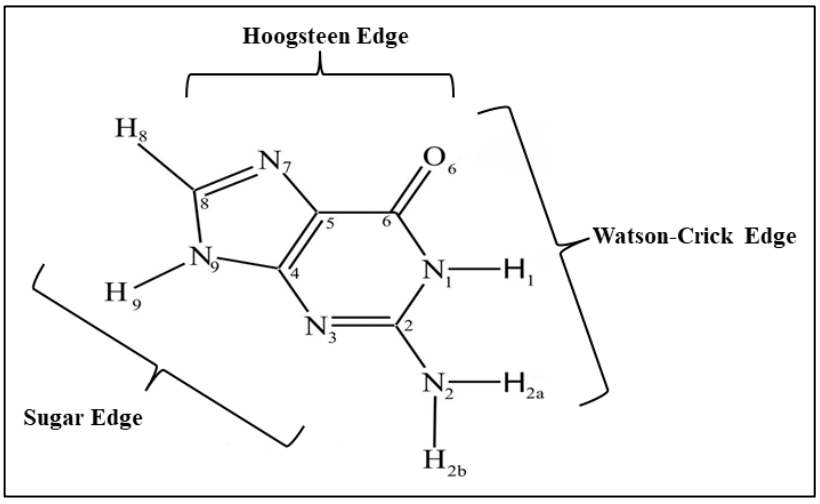

Figure 2.3: Bonding Sides of a Guanine Base

G4 structures build up within repetitive guanine rich regions of the human genome where each of the guanine bases forms two Hoogsteen hydrogen bonds with two adjacent guanine bases. This type of bond forms within the N^1, N^2, N^7 and O^6 locations of the four guanine bases. This means that four guanine bases can associate through eight Hoogsteen hydrogen bonds to form a planar ring structure called a guanine tetrad (G-tetrad). Figure 2.4 illustrates a guanine tetrad. The eight Hoogsteen

hydrogen bonds between four guanine bases are indicated with dashed lines. This planar structure results in strong van der Waals attractions due to the large planar surfaces which in turn causes the tetramers to get stuck on top of each other forming the G4 structure [24, 25, 26].

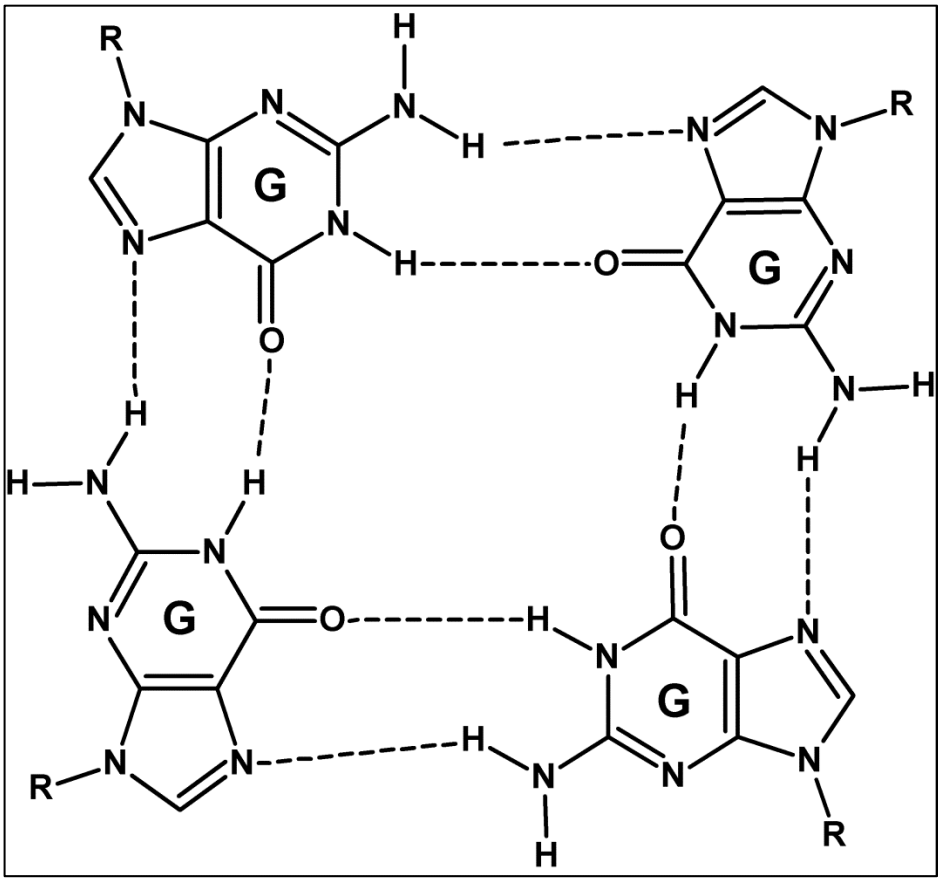

Figure 2.4: Guanine Tetrad

G4 structures are classified according to the number of strands involved in its formation. That is, the intermolecular type forms by the interactions of two or more strands. On the other hand, the intramolecular G4 structure forms as a result of the folding of a single strand [26]. Figure 2.5 illustrates the types of G4 structures [25]. The squares and the arrows represent the G-tetrads and the direction of the strands, respectively.

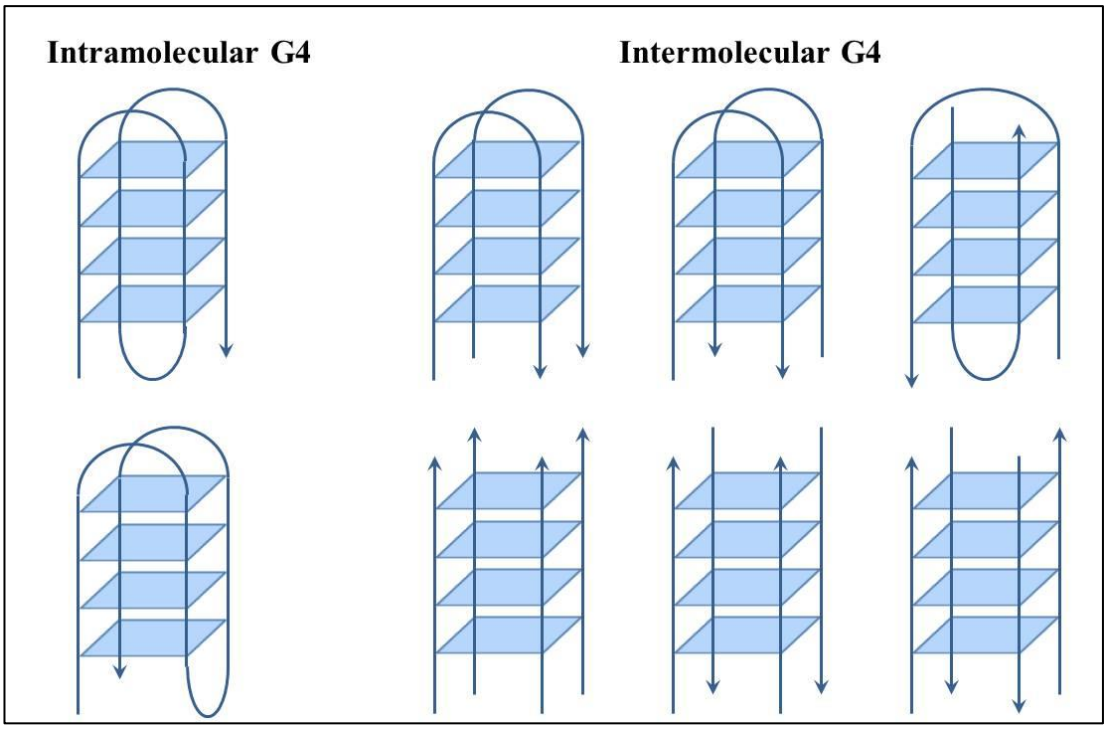

Figure 2.5: Intermolecular and Intramolecular G-quadruplex Structures

The DNA strand as well as the environmental conditions such as the temperature or pH has an influence on the conformation of the G4 structure. Investigation about which type of structure is formed could be done by the aid of electrophoretic separation technique. It is supposed that the bands that migrate faster are intramolecular structures. On the other hand, bands that migrate slower belong to intermolecular structures that contain several strands. Moreover, the migration of the DNA sample could also be attributed to the sequence itself, its conformation, the molecular weight and the protocol used for annealing [27].

G4 structures have been reported throughout important regions of the eukaryotic genome such as the telomeres and promoter regions of humans [13], the promoter of the chicken beta globin gene [28] and in living cells [29].

2.2 G-Quadruplex Structures in Human DNA

2.2.1 Human Telomeres

Telomeres are located at the end of chromosomes. Telomeres of higher organisms are known to contain a short tandem repeat. In humans, this is a hexameric (6 base pair long) tandem repeat and the sequence is TTAGGG in the 5' to 3' direction [30]. It is mostly found in duplex form however, it ends in a 3' single stranded overhang which acts like a cap protecting the ends of chromosomes and also prevents end to end fusion [31].

Chromosomes shorten with each cycle of DNA replication [32]. The telomerase enzyme maintains the length of chromosomes by adding telomeric repeat sequences to assure that telomere shortening does not occur [33]. The telomerase enzyme is not active in somatic cells, however it is active in most human tumors and this is what makes the telomeres a target for the study of cancer therapies. The expression of the telomerase enzyme in human tumors prevents the cells from entering senescence [34], therefore one way to inhibit cancer cells from growing up to an infinite number would therefore be suppressing the activity of the telomerase enzyme [35].

The 3' single stranded overhang with the TTAGGG tandem repeat is a region which is uniquely rich in repetitive guanine bases [36]. As mentioned earlier, G4 structures were reported throughout the human telomeres due to this richness in guanine [13]. Scientists are working on G4 ligands that can induce G4 structures at the 3' single strand overhang of telomeres in order to decrease the activity of telomerase [6].

2.2.2 Promoter Regions

The human genome was found to contain more than 300,000 G4 forming sequences according to the results of a genome-wide bioinformatics investigation performed in

2005. The abundance of those unusual secondary structures is not just by chance, but some regions of the genome are specifically rich in G4 structures [37]. Apart from the human telomeric regions that were discussed earlier, promoter regions of genes that are attributed to cancer are characterized with their G4 forming potential [38].

Oncogenes with guanine rich promoter regions that were reported previously include c-kit [39], which is going to be used in this thesis, c-myc [40] the human vascular endothelial growth factor (VEGF) [40] and the human telomerase reverse transcriptase (hTERT) [38]. The presence of G4 forming sequences in the promoter regions of oncogenes suggests their important roles in the regulation of transcription of oncogenes [42]. Organic molecules such as perylene derivatives have been reported to induce the formation of G4 structures on the promoter region of the VEGF gene and play a role as transcriptional repressor in cancer cell lines [5].

2.2.3 Beta Globin Gene Promoter

According to an investigation done previously, it was demonstrated that the chicken beta globin gene contains a region which could form a tetraplex structure in a potassium ion dependent way. This region forms a tetraplex structure with a complex conformation because it is stated that the sequence does not contain the regular four tandem guanine bases observed in other tetraplex structures. This was an *in vitro* study to stop DNA replication by acting like an obstruction to DNA polymerase suggesting that this could be the reason for recombination in this region possibly due to exchange of strands. In the absence of potassium ions, G4 structures are not formed in vitro and replication is not prevented. On the other hand, in the presence of potassium ions, a stable tetraplex is formed with non-guanine bases getting incorporated into the complex structure and this hinders DNA synthesis from taking place *in vitro* [43].

Chicken and human DNA show homology in beta globin locus control region and this was shown by Reitman et al. when they have found that there are elements in the human beta globin gene that resemble the elements in the chicken beta globin gene [44].

In this thesis, a repetitive guanine rich region of the human beta globin gene with the regular four tandem guanine bases (exon I, exon II and 60 bp of intron II after exon II) has been amplified by PCR and tested for the formation of G4 structures.

2.3 Molecules Able to Induce and Stabilize G-Quadruplex Structures

G4 ligands have been studied extensively due to their potential application as anticancer drugs. Previously, monovalent ions were studied for their G4 stabilizing potential by the aid of several spectroscopic measurements. Results indicated that both sodium and potassium ions play roles in stabilizing G4 structures. The conformation and molecularity were determined with respect to both types of ions used and their concentrations. Intermolecular G4 structures are favored when the monovalent ion is present at high concentration and there is only one or two nucleotides separating the guanine repeats [27].

Furthermore, there are several classes of organic molecules that were also extensively studied with regard to their G4 formation and stabilization potential and they were found to have some common characteristics. The first and the most notable property is that all of the organic molecules used for this purpose share a large aromatic core. This is necessary for the stacking interactions with the guanine tetrads. Secondly, they possess side chains preferably with a positive charge. This is

required for the interactions with the negatively charged DNA grooves or to increase the solubility of the molecule [15, 45]. Thirdly, those molecules mostly own good water solubility and high fluorescence quantum yield in water and this is critical because drug design needs further investigation in cell lines [9].

Organic molecules studied for their G4 binding selectivity include perylene dyes [33, 40], naphthalene dyes [46], porphyrins [47], isoalloxazines [12], coronenes [48] and telomestatin [49].

2.4 Perylene Derivatives

Perylene derivatives are among the most famous molecules used for those kind of studies. The wide range of applications of perylene derivatives is because of their adjustable properties with regard to their area of application[50].

By the aid of this advantage, perylene derivatives could be modified by producing symmetrical or unsymmetrical analogues [6, 51], enlarging their cores [52] or by adding charged or uncharged, long or short, weakly or strongly basic [15] substituents to them. For example, synthesizing perylene tetracarboxylic dianhydrides (PDAs) and perylene diimides (PDIs) with appropriate substituents at the perylene core and imide position could enhance their solubility [50]. This might make perylene dyes good intercalators with the negatively charged backbone of DNA. Those enhancing strategies actually prove that in the near future it should be possible to engineer perylene derivatives that will work as G4 binding ligands and promise to be a chemotherapy based on telomeres and oncogenes [53].

2.5 Ligand Interactions with G-Quadruplex DNA

A ligand that would be used for G4 binding studies should preferentially identify the structure with high specificity as well as affinity. There are a number of methods used for the investigation of interactions between the G4 structure and the ligand and each technique is characterized by its own benefits and drawbacks [54].

As mentioned earlier, the telomeric regions as well as the promoter regions of oncogenes are rich in guanine bases and have a potential to form G4 structure. Therefore ligands can attenuate telomerase activity either by preventing telomerase from accessing its substrate or by downregulating hTERT expression at the hTERT promoter [6].

While binding of ligands to G4 structures has been well investigated, the mechanism of binding remains unclear and complicated [55]. Different ligands and side chains recognize the G4 structures in different ways and have different binding modes as well as stoichiometry towards them [56, 57]. There are several principles by which ligands bind to G4 structures: 1) Interaction with the top or bottom external G-tetrads through π- π interactions [52]. 2) Interaction with the loops or the grooves by hydrogen bonding or electrostatic interaction [56]. 3) Intercalation between G-tetrads. This mechanism needs high energy because the ligand should distort the G4 structure [58]. Aromatic compounds have a large planar aromatic core that favors π-π interactions via the external G-tetrads. If the compound possesses side chains as well, they will surround the G4 structure in a way that resembles an anchor [55].

While some ligands interact with only one of the modes described above, some others use more than one binding mode [54]. Binding modes of ligands to G4

structures are shown in Figure 2.6. The squares represent the G-tetrads, the arrows represent the direction of the strands and the red oval shape represents the G4 ligands [59].

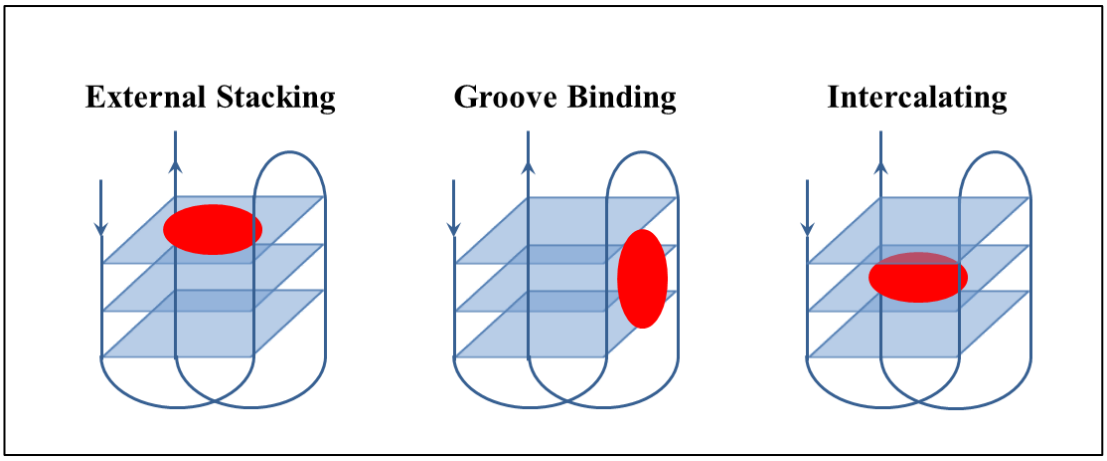

Figure 2.6: Binding Modes of Ligands to G-quadruplexes

Chapter 3

EXPERIMENTAL

3.1 Materials

1,7-di(3,5-diamino-pyrimidoxyl)perylene-3,4,9,10-tetracarboxylic dianhydride (YPDA) and 1,7-di(thiazolium)perylene-3,4,9,10-tetracarboxylic dianhydride (CPDA) were synthesized by Moustafanejad M. and N,N'-bis(4-benzosulfonic acid)perylene-3,4,9,10-tetracarboxylic diimide (SPDI) was synthesized by Pasaogullari N. earlier and the FT-IR spectra for each compound is provided in Chapter 4 (Figures 4.1, 4.2, and 4.3).

The DNA oligonucleotides were purchased from Oligomer Biyoteknoloji (Çankaya, Ankara) and used without further purification. The sequences of the seven oligonucleotides are shown in Table 1.1. The Blirt 50X Tris-acetate-EDTA (TAE) buffer, Blirt 2xPCR TaqNova-Red - $_{M}$aster mix with Taq polymerase (RP85T), Blirt 2'-deoxynucleoside 5'-triphosphates (dNTPs) mix and Blirt Extractme DNA clean-up & gel-out kit were purchased from En-Ergon Scientific (Nicosia, Cyprus). Biorad 5x Orange G Loading Dye, Biorad Genes in a Bottle Lysis Buffer, Axygen 100 bp DNA ladder, Invitrogen UltraPure™ Agarose, Thermo Scientific Proteinase K and pure alcohol were used.

3.2 Instruments

Ultraviolet Absorption Spectrometer

All the spectra were investigated in Tris-HCl buffer using a Varian Cary-100 Spectrophotometer.

Emission Spectrometer

All the spectra were investigated in Tris-HCl buffer using a Varian Cary Eclipse Spectrophotometer.

Bandelin Electronic Soronex RK 52H Bath

The compounds were allowed to dissolve in Tris-HCl with the aid of Bandelin Electronic Soronex RK 52H Bath.

Tanon HE-120 horizontal gel electrophoresis

The agarose gels were run by Tanon HE-120 horizontal gel electrophoresis.

Tanon EPS-300 Power Supply

All gels were run via Tanon EPS-300 Power Supply.

J.P. Selecta Centrofriger-BL-II

Gel-out protocol was carried out with the aid of J.P. Selecta Centrofriger-BL-II.

Bioer Life Express PCR Machine

PCR were carried out with the Bioer Life Express PCR Machine.

Bioer Mixing Block MB-102

Incubations were carried out with the aid of Bioer Mixing Block MB-102.

Gel Documentation & Analysis System - Beijing Liuyi Instrument Factory

All agarose gels were visualized with Gel Documentation & Analysis System.

OHAUS Balance

Weight measurements were carried out with the aid of OHAUS Balance.

Bandelin Electronic Soronex RK 52H Bath

DNA extraction protocol was carried out with the aid of Bandelin Electronic Soronex RK 52H Bath.

Electrolux Heatwave Compact Quartzgrill 1000W

Agarose gels were prepared with the aid of Electrolux Heatwave Compact Quartzgrill 1000W.

3.3 Methods

3.3.1 Preparation of Compound Solutions in Tris-HCl Buffer

Initially, 100 μM stock solution of each compound SPDI, YPDA and CPDA was prepared in 1M Tris-HCl buffer solution at pH 7.4 according to Equation 3.1 (Eqn. 3.1). The solutions of the compounds in Tris-HCl buffer were then put in the sonicator at room temperature for 1 hour for maximum dissolution. 2.5 μM, 5 μM, 10 μM and 20 μM concentrations of the perylene derivatives were then prepared by serial dilutions from the stock solution.

$$m = M \times M_w \times V \qquad \text{(Eqn. 3.1)}$$

Where,

m: Mass of the compound

M: Molarity

M_w: Molecular weight of the compound

V: Volume of solution

3.3.2 Absorption (UV-vis) Spectroscopy

Absorption measurements of the pure compounds (20 μM) and pure primers (20 μM) were done in 1M Tris-HCl buffer at pH 7.4. Measurements were taken at different time intervals for pure compounds taking care not to disturb the particles (shake the cuvettes) between measurements in order to observe their aggregation. 0 hour (0h) refers to the spectrum measured immediately after the pure compound solution was removed from the sonicator (1 hour at room temperature). 1hour (1h), 3 hours (3h), 6 hours (6h), 24 hours (24h) and 48 hours (48h) refer to the spectra measured after the pure compound solution was left undisturbed at room temperature and darkness.

Absorption measurements of the primer and compound complexes were done in a 1:1 ratio of concentration and 1:10 ratio of volume and after 3 hours of incubation at room temperature and darkness without any disturbance.

3.3.3 Emission Spectroscopy

Emission measurements of the pure compounds (20 μM) and pure primers (20 μM) were done in 1M Tris-HCl buffer at pH 7.4. Measurements were taken at different time intervals for the pure compounds taking care not to disturb the particles between measurements. 0 hour (0h) refers to the spectrum measured immediately after the pure compound solution was removed from the sonicator (1 hour at room temperature). 1hour (1h), 3 hours (3h), 6 hours (6h), 24 hours (24h) and 48 hours (48h) refer to the spectra measured after the pure compound solution was left undisturbed at room temperature and darkness.

Emission measurements of the primer and compound complexes were done in a 1:1 ratio of concentration and 1:10 ratio of volume and after 3 hours of incubation at room temperature and darkness without any disturbance. Emission measurements for the pure compounds and for the primer and compound complexes were carried out at λ_{exc}= 485 nm and emission measurements for the pure primers were carried out at λ_{exc}= 250 nm.

3.3.4 DNA Extraction

The DNA extraction protocol was carried out with permission from the Eastern Mediterranean University Research and Publication Ethics Board. The permission letter is provided at the end of this thesis. The inside of the cheeks were chewed well, paying attention not to bleed, for 1 minute with 3 mL of distilled water and then the liquid was expelled back into a clean falcon tube. 2 mL of lysis buffer was added to the same tube and it was inverted a few times gently. Proteinase K solution (100 mg in 1 mL) was added and the tube was inverted again. The tube containing the liquid was incubated at 50 ℃ in a water bath for 10 minutes and after that cold alcohol was added slowly. Inverting the tubes again after a while also allowed DNA to aggregate before it was collected in a separate Eppendorf tube. Figure 3.1 illustrates the isolated human DNA.

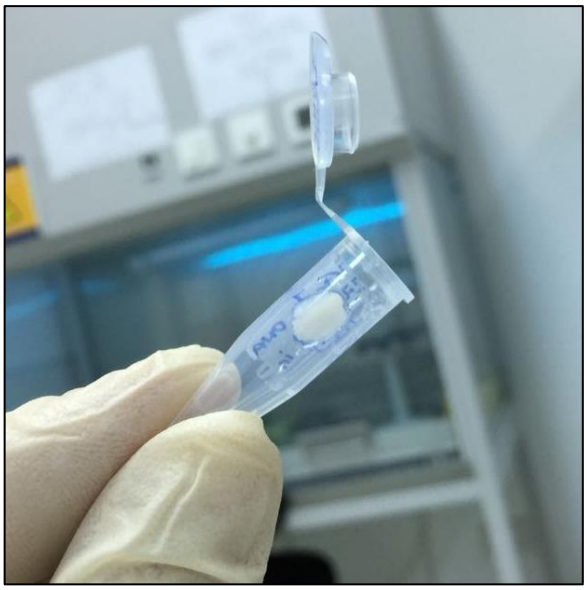

Figure 3.1: The Isolated Human DNA

3.3.5 Polymerase Chain Reaction (PCR)

Polymerase Chain Reaction (PCR) [17, 18] was carried out for a guanine rich region of the beta globin gene (exon I, exon II and 60 bp of intron II after exon II) from the isolated human DNA. Figure 3.2 illustrates the amplified region with the location of the forward and reverse primers.

Homo sapiens chromosome 11, GRCh38.p7 Primary Assembly
NCBI Reference Sequence: NC_000011.10

Forward Primer (PCO3)

ACATTTGCTTCTGACACAACTGTGTTCACTAGCAACCTCAAACAGACACCATGGTGCATCTGACTCCTGA
GGAGAAGTCTGCCGTTACTGCCCTGTGGGGCAAGGTGAACGTGGATGAAGTTGGTGGTGAGGCCCTGGGC
AGGTTGGTATCAAGGTTACAAGACAGGTTTAAGGAGACCAATAGAAACTGGGCATGTGGAGACAGAGAAG
ACTCTTGGGTTTCTGATAGGCACTGACTCTCTCTGCCTATTGGTCTATTTTCCCACCCTTAGGCTGCTGG
TGGTCTACCCTTGGACCCAGAGGTTCTTTGAGTCCTTTGGGGATCTGTCCACTCCTGATGCTGTTATGGG
CAACCCTAAGGTGAAGGCTCATGGCAAGAAAGTGCTCGGTGCCTTTAGTGATGGCCTGGCTCACCTGGAC
AACCTCAAGGGCACCTTTGCCACACTGAGTGAGCTGCACTGTGACAAGCTGCACGTGGATCCTGAGAACT
TCAGGGTGAGTCTATGGGACGCTTGATGTTTTCTTTCCCCTTCTTTTCTATGGTTAAGTTCATGTCATAG
GAAGGGGATAAGTAACAGGGTACAGTTTAGAATGGGAAACAGACGAATGATTGCATCAGTGTGGAAGTCT

Reverse Primer (CD6)

Figure 3.2: The Amplified Region of the Beta Globin Gene

All the reagents used for the PCR reaction are provided in Table 3.1. The PCR buffer, Taq polymerase, dNTP mix, forward (PCO3) and reverse (CD6) primers and H_2O which make up the master mix were added to the DNA template. The PCR tubes were then placed in the thermal cycler. Initial denaturation was carried out at 94 ℃ for 2 minutes followed by denaturation at 94 ℃ for 30 seconds. Annealing of the primers to the DNA was allowed by decreasing the temperature to 57 ℃ for 30 seconds. The elongation step, amplification of the DNA template by the DNA polymerase, was performed for 1 minute at 68 ℃. This made up a total of 30 cycles. The conditions for PCR are provided in Table 3.2. 1% agarose gel (1 g in 1X TAE buffer) was then loaded with 5 µl of 100 bp DNA ladder and 3 µL of Orange G loading dye and 10 µL of the PCR sample and 10 µL of Orange G loading dye. The gel was run at 150 volt (150V) for 1 hour. The image of the gel is shown in Figure 4.26 **A**.

Table 3.1: Components and Amounts of the PCR Reaction

Components	**Final Concentration**	**Volume**	**Total Volume (10 Reactions)**
10X PCR Buffer	1X	5 µL	55 µL
Taq Polymerase 5 u/µL	1 u	0.2 µL	2.2 µL
Forward Primer (PC03) T_m=55 ℃ 100 µM	10 pmol	1 µL	11 µL
Reverse Primer (CD6) T_m=58 ℃ 100 µM	10 pmol	1 µL	11 µL
dNTP mix (10 mM each)	0.2 mM	1 µL	11 µL
DNA template	0.5 µg	1 µL	11 µL
H_2O	–	40.8 µL	448.8 µL
Total	50 µL	50 µL	550 µL

Table 3.2: PCR Conditions

	Temperature	**Duration**
	94 ℃	2 minutes
35 Cycles	94 ℃	30 seconds
	57 ℃	30 seconds
	68 ℃	1 minute
	4 ℃	HOLD

3.3.6 Gel-Out Protocol

The region with the PCR product was excised from the agarose gel in order to carry out the gel-out protocol. Figure 4.26 **B** shows an image of the gel after it was excised. The gel-out protocol was carried out according to the manufacturer's protocol.

3.3.7 G-Quadruplex Formation Assay

4% agarose gel (4g in 100mL 1X TAE buffer) was prepared. Each perylene derivative was added to the PCR product and 3μL of Orange G loading dye, and the complex was immediately loaded into the gel. The gel was loaded with the perylene derivative and the eluted PCR product starting with a 1:1 ratio of concentration and then applying two-fold dilution to the concentration of the perylene derivative. The order of the wells (wells 1 to 13 in Fig. 4.27) from left to right and the amount loaded to each well is provided in Table 3.3. The gel was run at 150V for 2 hours. The image of the gel under UV light is provided in Figure 4.27.

Table 3.3: Order of the Wells in Agarose Gel (Fig. 4.27)

Well Number	Samples Loaded
Well 1	100 bp DNA Ladder (5 μL)
Well 2	PCR product alone (10 μL)
Well 3	PCR product (10 μL) + 2.5 μM SPDI (10 μL)
Well 4	PCR product (10 μL) + 5 μM SPDI (10 μL)
Well 5	PCR product (10 μL) + 10 μM SPDI (10 μL)
Well 6	PCR product (10 μL) + 2.5 μM YPDI (10 μL)
Well 7	PCR product (10 μL) + 5 μM YPDI (10 μL)
Well 8	PCR product (10 μL) + 10 μM YPDI (10 μL)
Well 9	PCR product (10 μL) + 2.5 μM CPDI (10 μL)
Well 10	PCR product (10 μL) + 5 μM CPDI (10 μL)
Well 11	PCR product (10 μL) + 10 μM CPDI (10 μL)
Well 12	PCR product alone (10 μL)
Well 13	100 bp DNA Ladder (5 μL)

Chapter 4

DATA

4.1 UV-visible and Emission Spectra

The results of the absorption and emission measurements of the pure primers, pure compounds and the complexes are provided below;

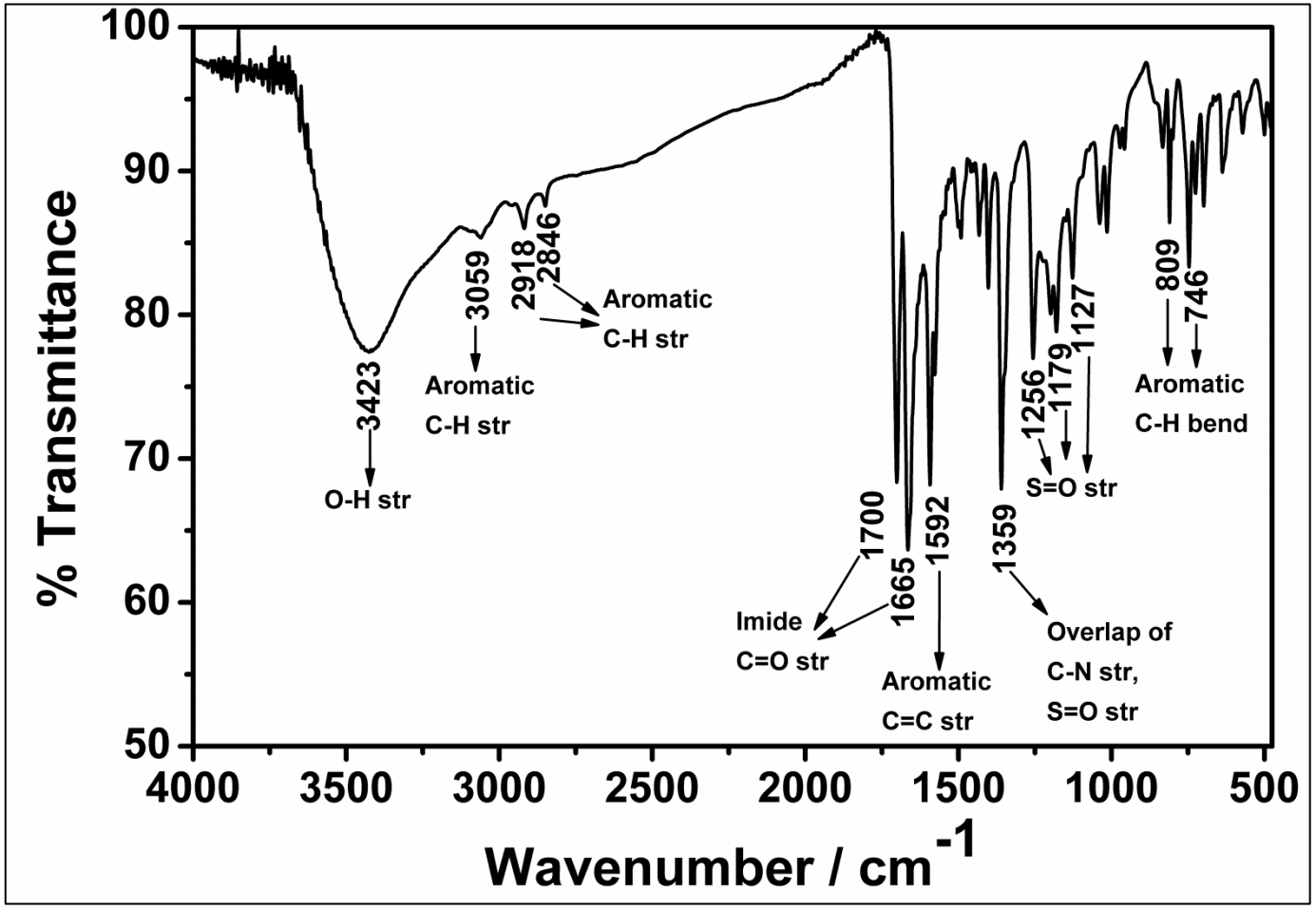

Figure 4.1: SPDI, Infrared Spectrum, KBr Pellet

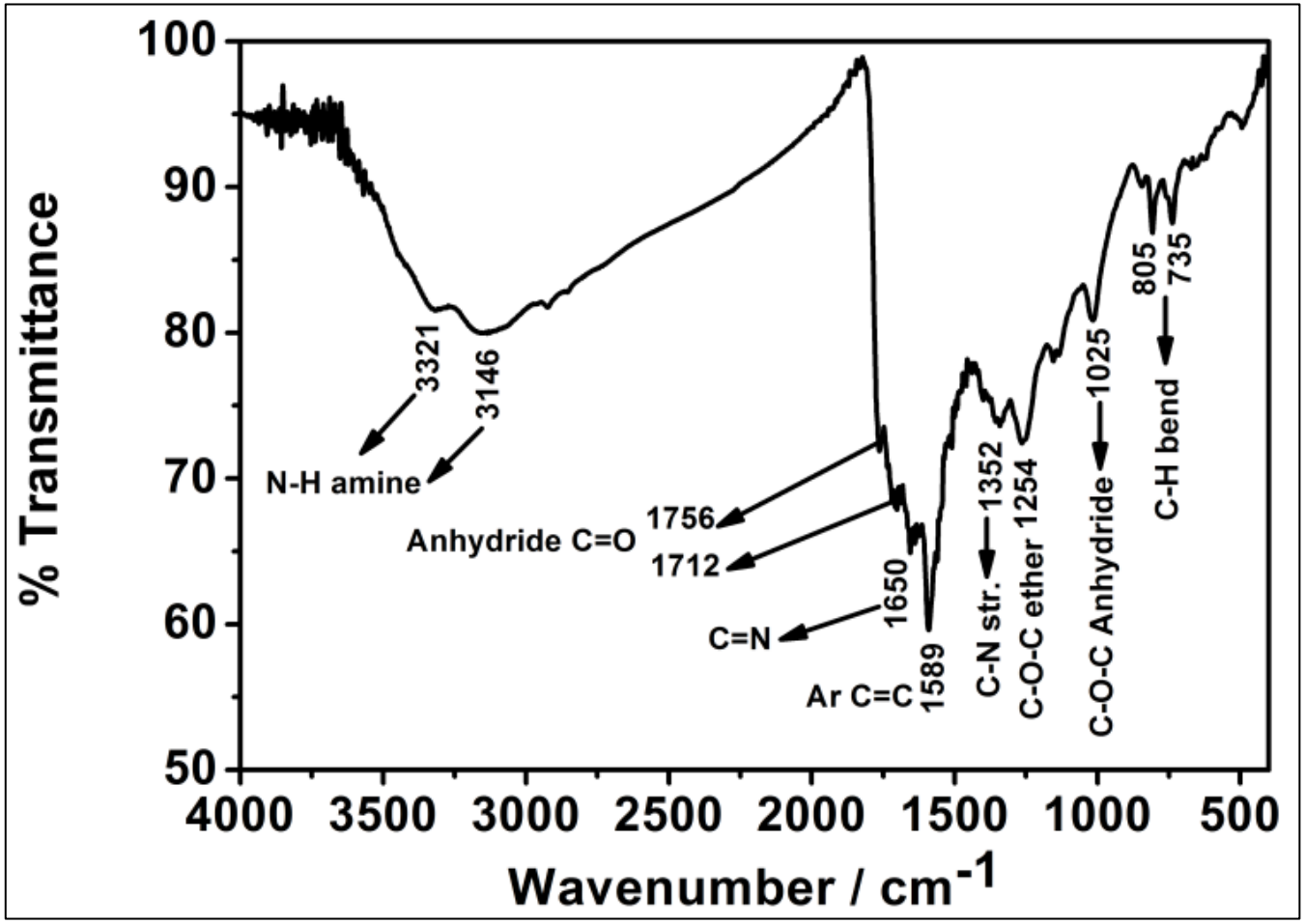

Figure 4.2: YPDA, Infrared Spectrum, KBr Pellet

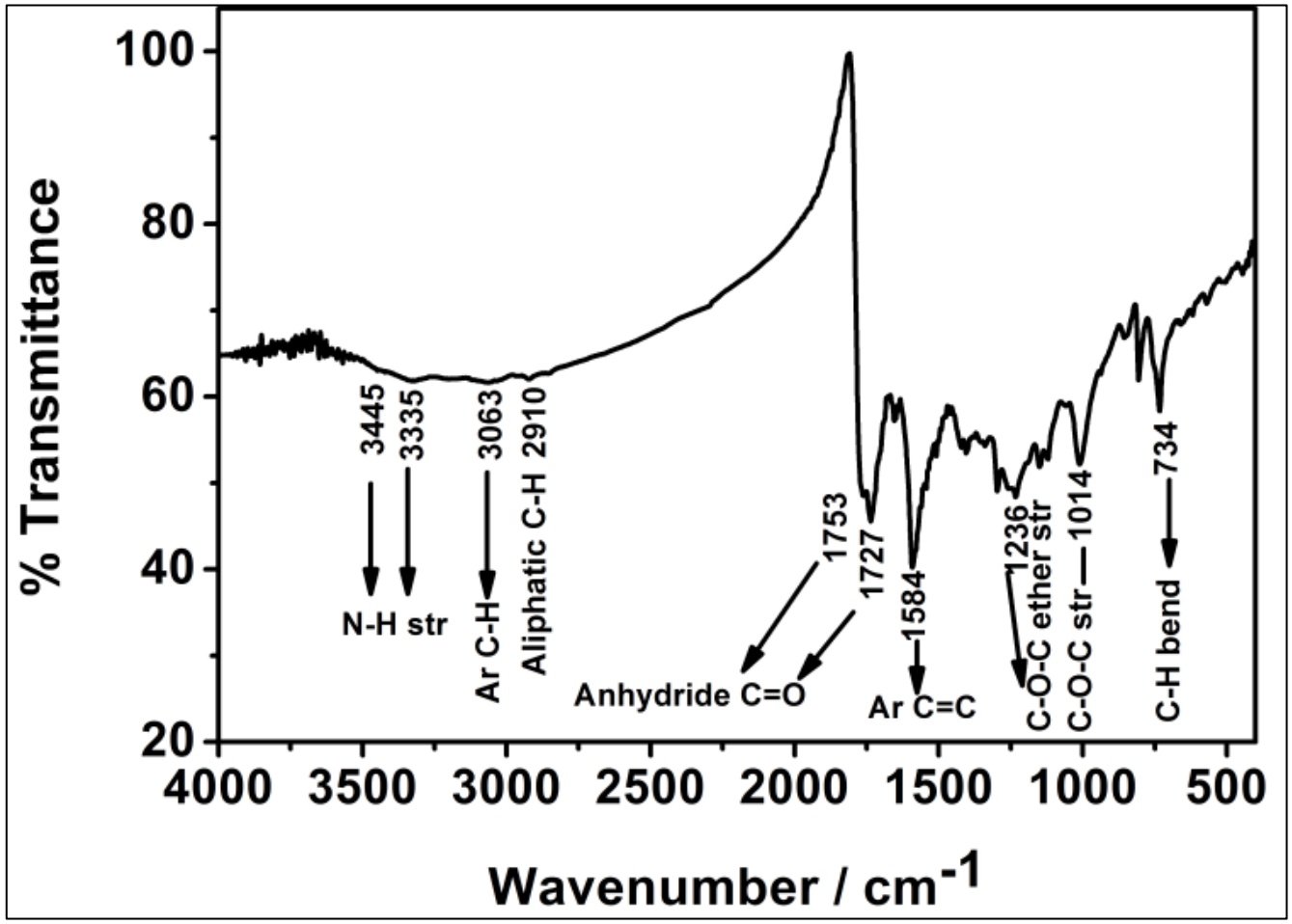

Figure 4.3: CPDA, Infrared Spectrum, KBr Pellet

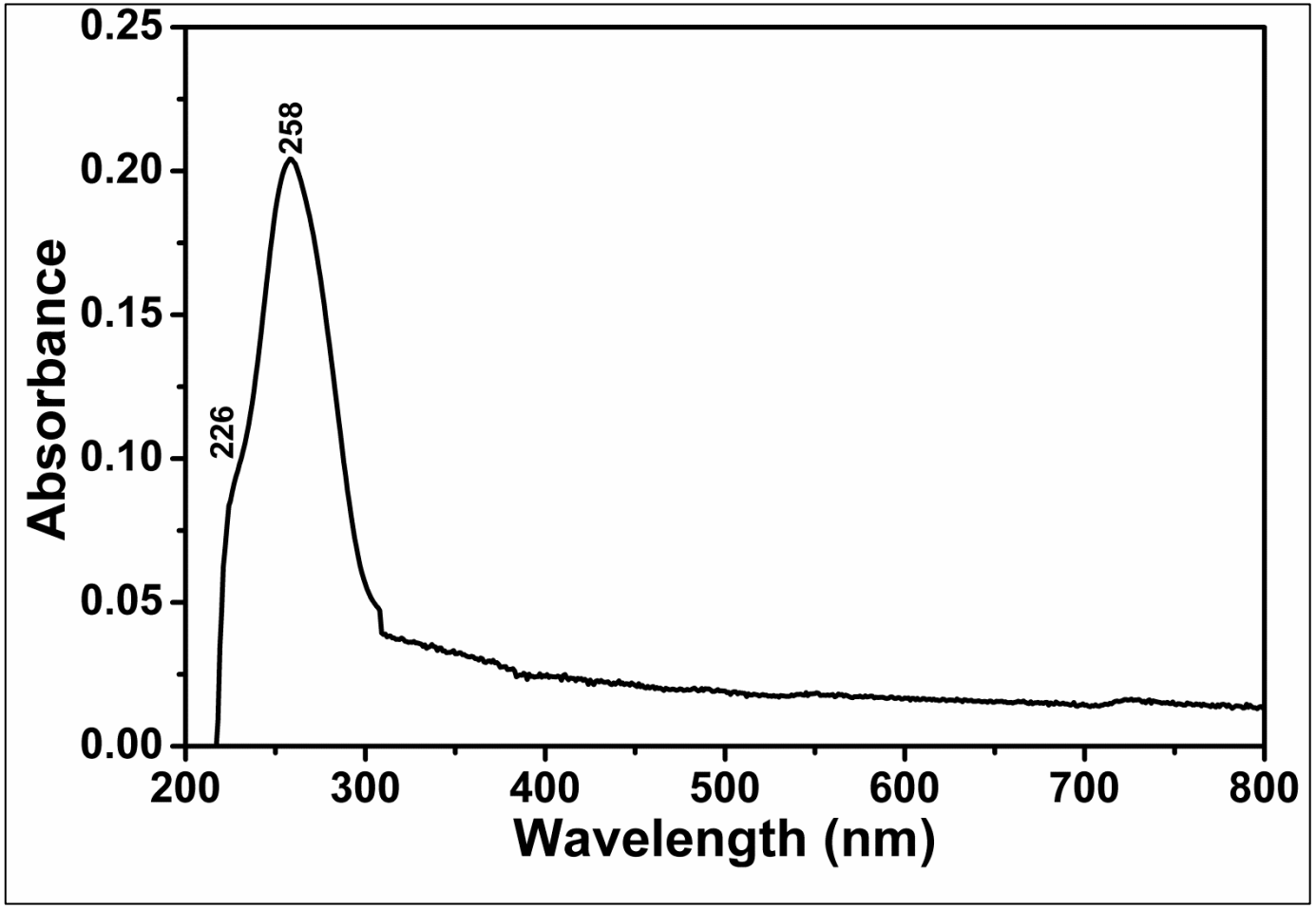

Figure 4.4: a-coreTT, Absorption Spectrum (1M Tris-HCl Buffer pH 7.4)

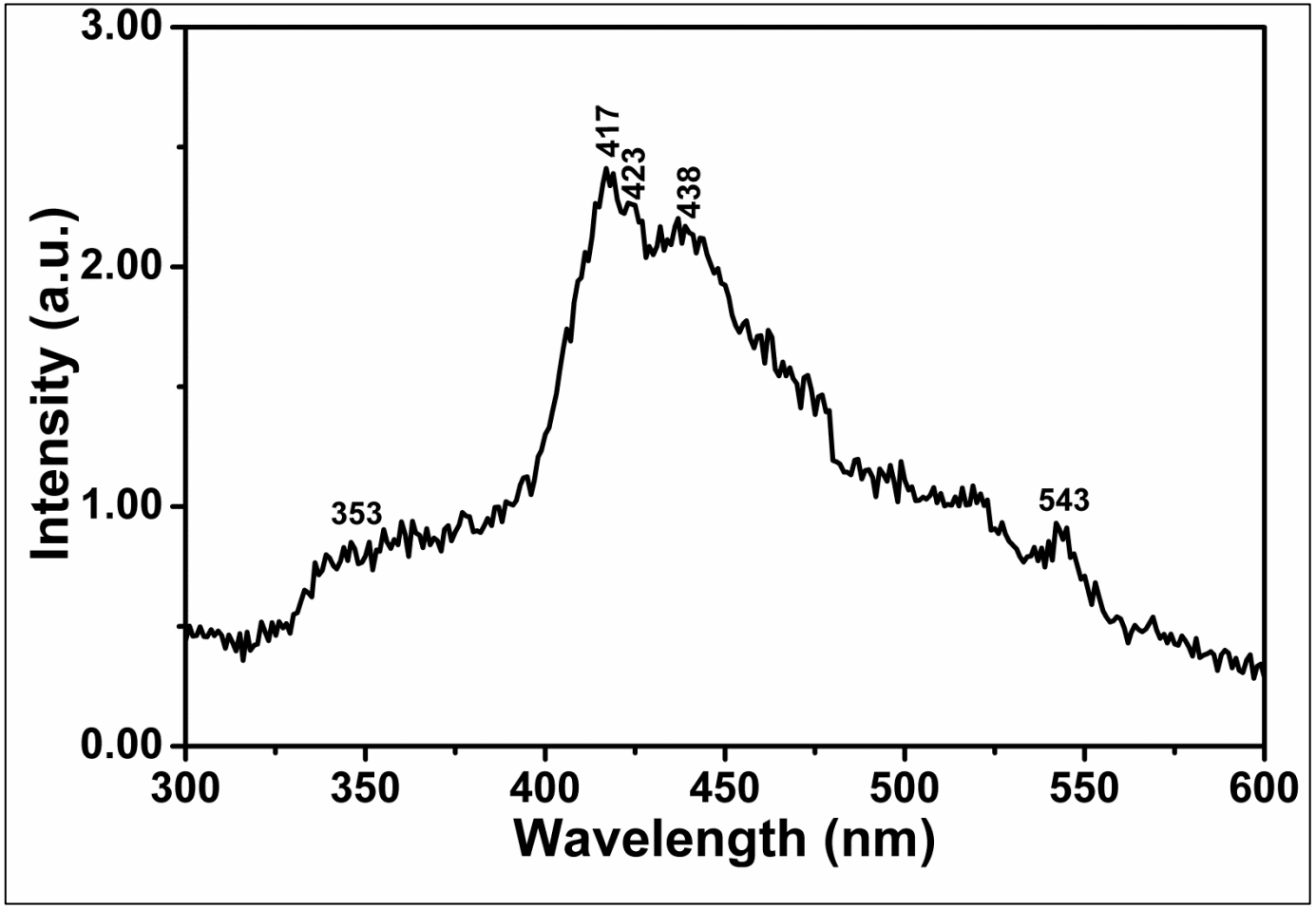

Figure 4.5: a-coreTT, Emission Spectrum (1M Tris-HCl Buffer pH 7.4)
(λ_{exc} = 220 nm)

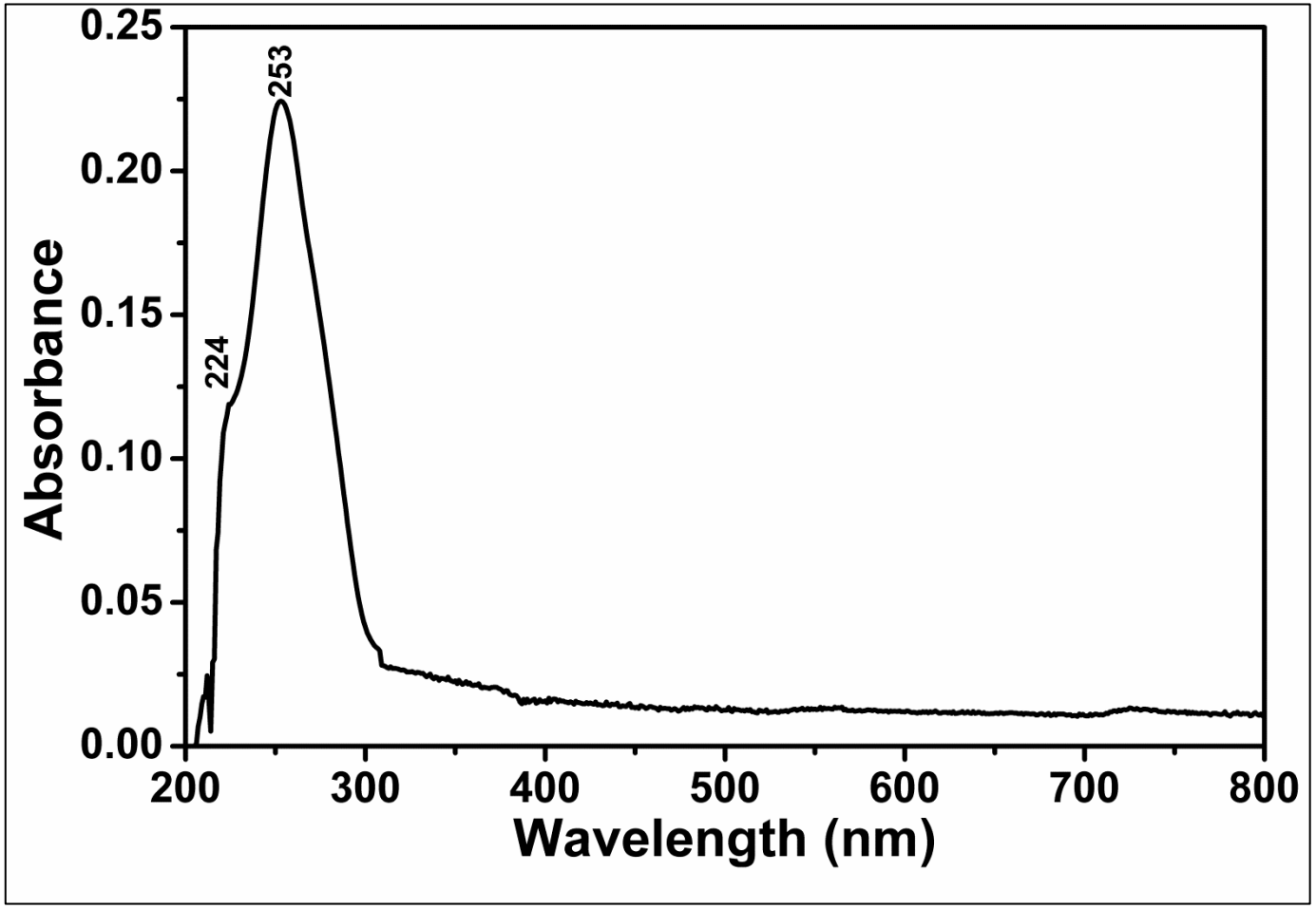

Figure 4.6: c-kit, Absorption Spectrum (1M Tris-HCl Buffer pH 7.4)

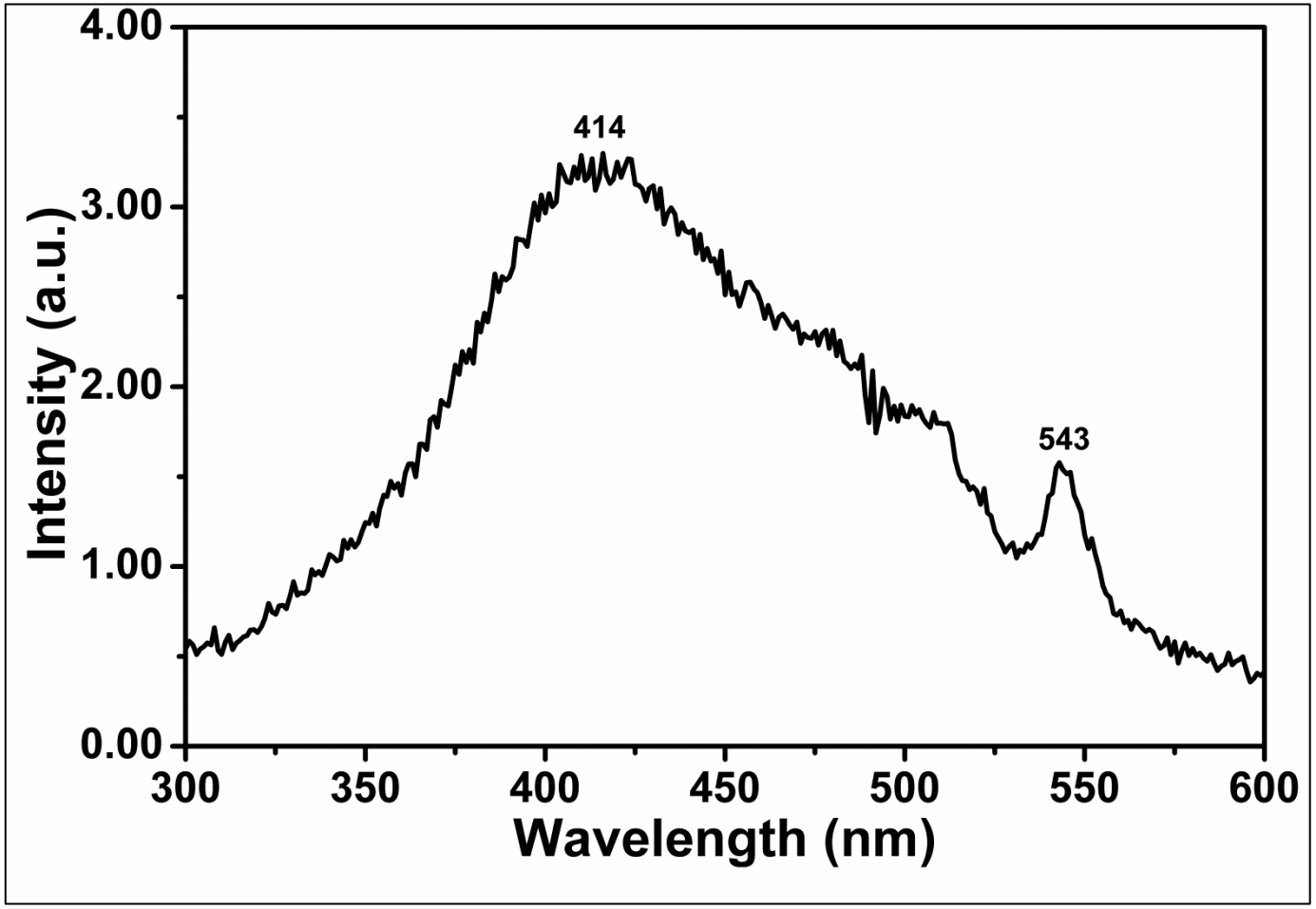

Figure 4.7: c-kit, Emission Spectrum (1M Tris-HCl Buffer pH 7.4)
(λ_{exc} = 220 nm)

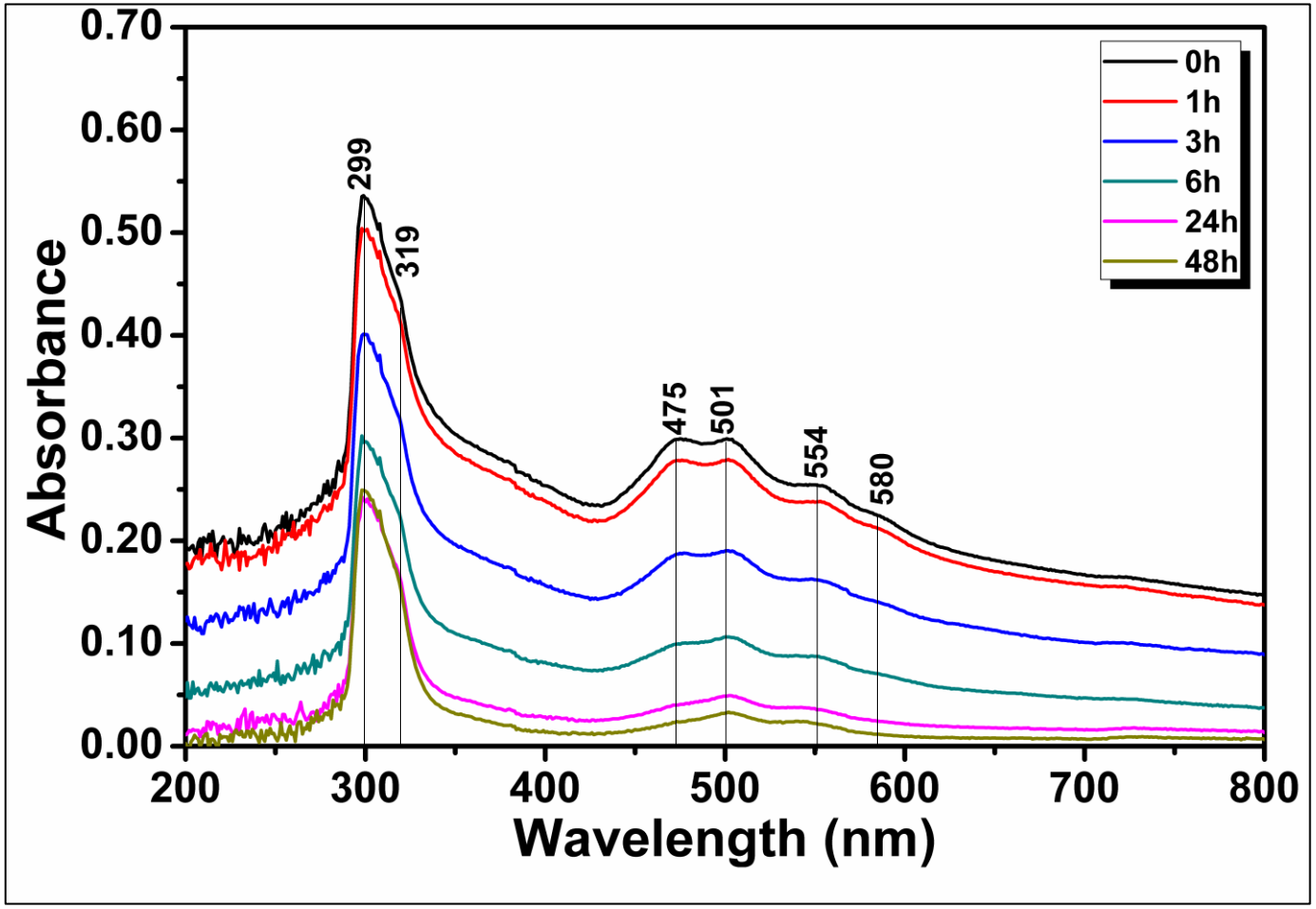

Figure 4.8: SPDI, Absorption Spectrum (1M Tris-HCl Buffer pH 7.4)

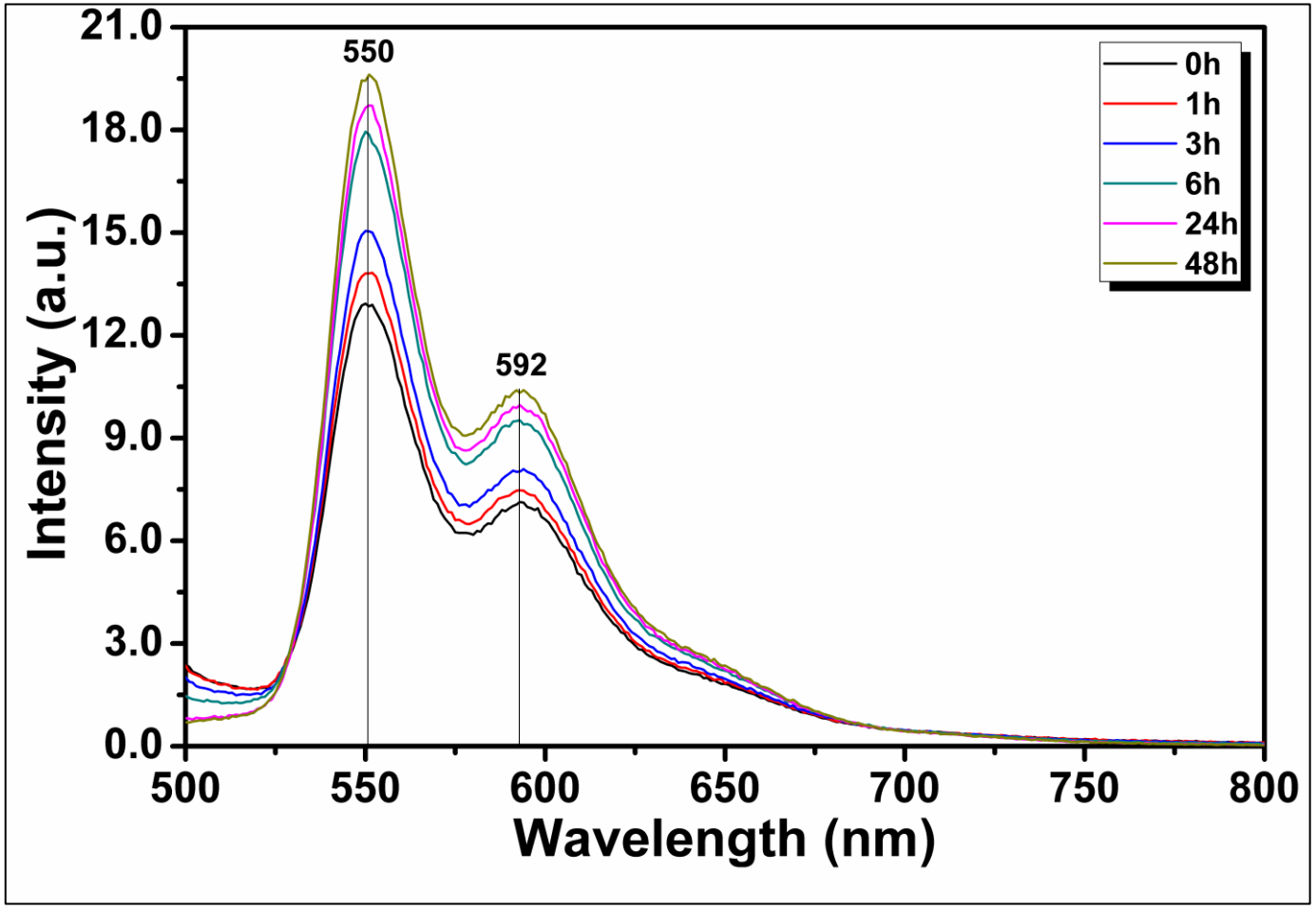

Figure 4.9: SPDI, Emission Spectrum (1M Tris-HCl Buffer pH 7.4)
(λ_{exc} = 485 nm)

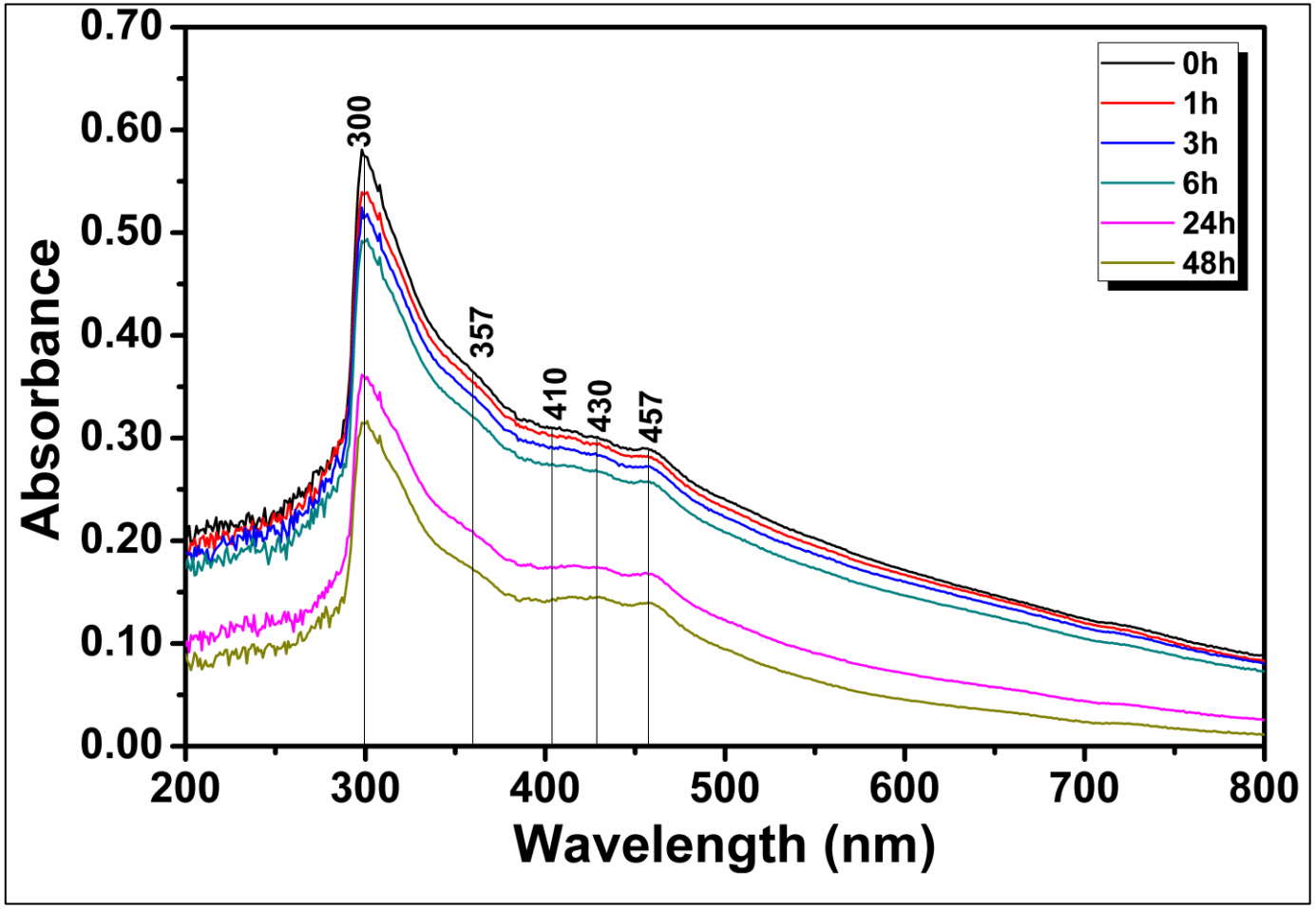

Figure 4.10: YPDA, Absorption Spectrum (1M Tris-HCl Buffer pH 7.4)

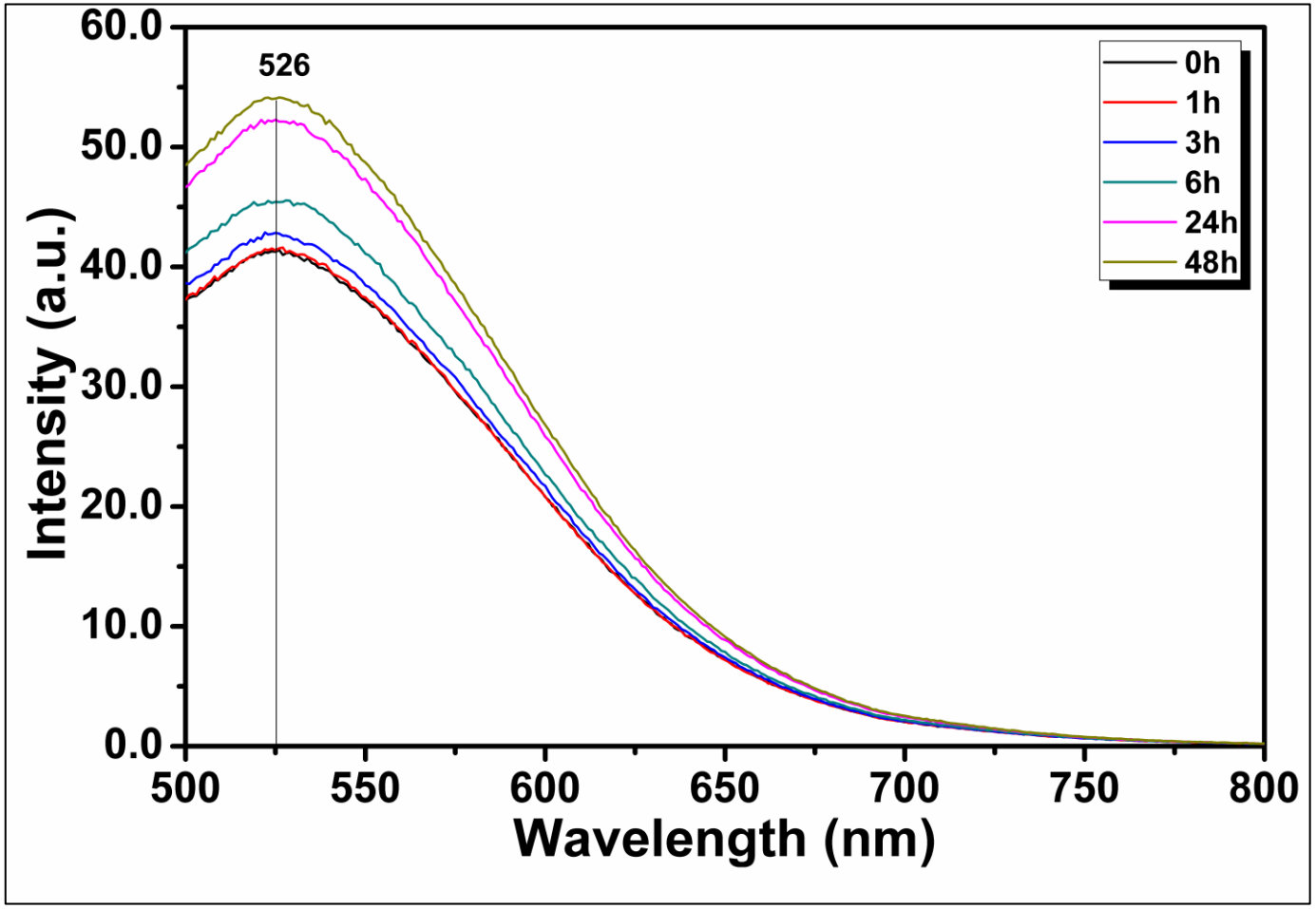

Figure 4.11: YPDA, Emission Spectrum (1M Tris-HCl Buffer pH 7.4)
(λ_{exc} = 485 nm)

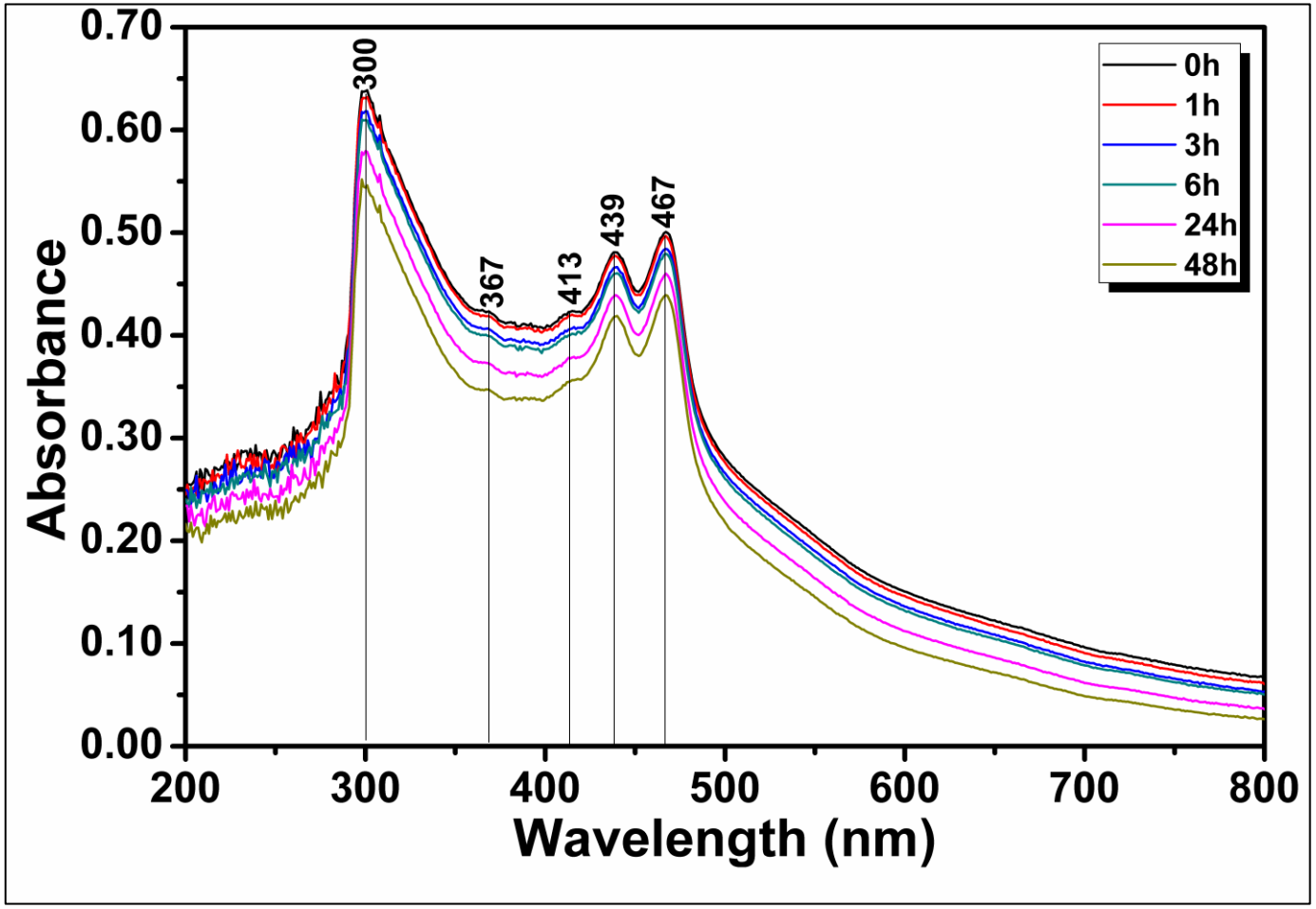

Figure 4.12: CPDA, Absorption Spectrum (1M Tris-HCl Buffer pH 7.4)

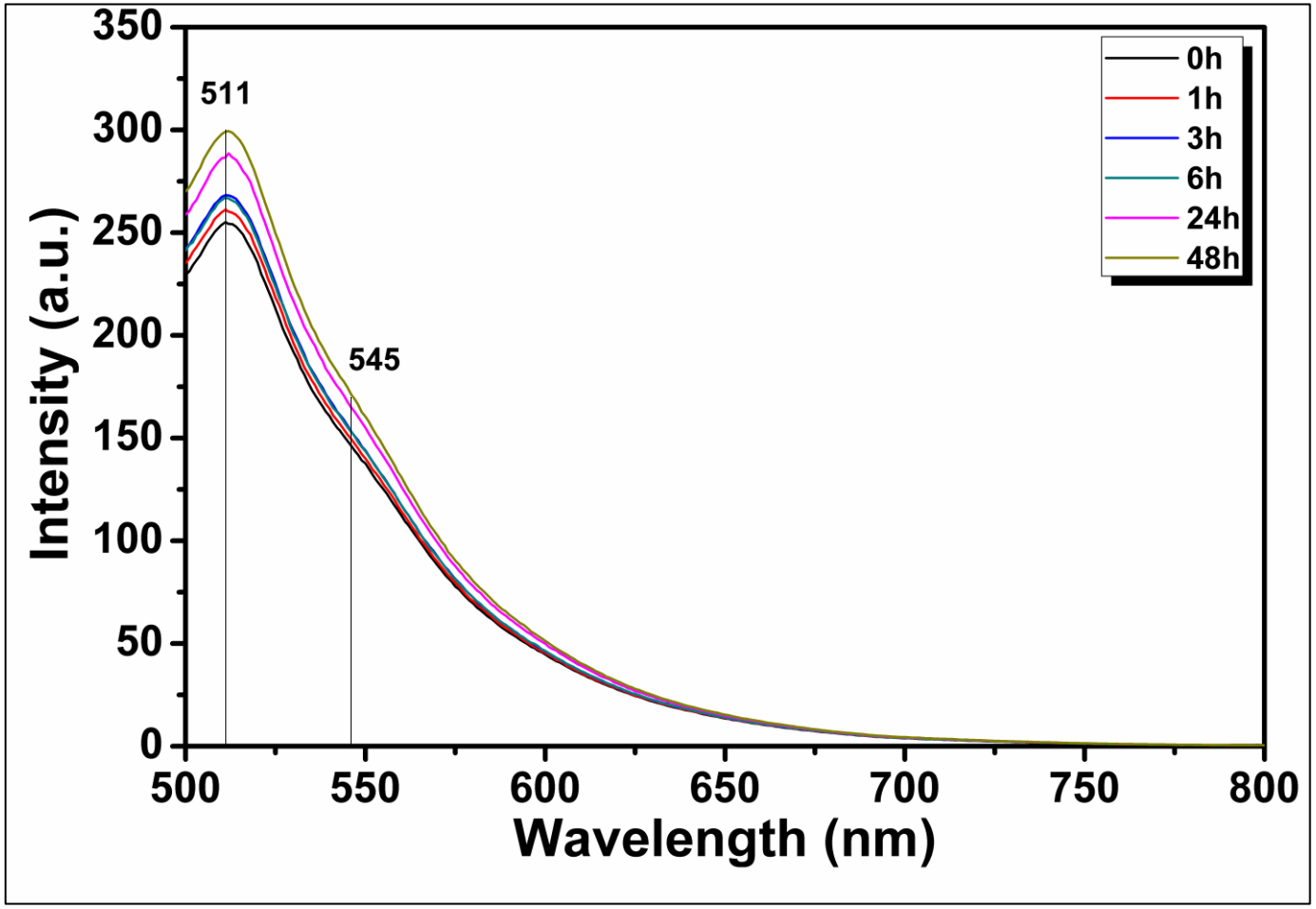

Figure 4.13: CPDA, Emission Spectrum (1M Tris-HCl Buffer pH 7.4)
(λ_{exc} = 485 nm)

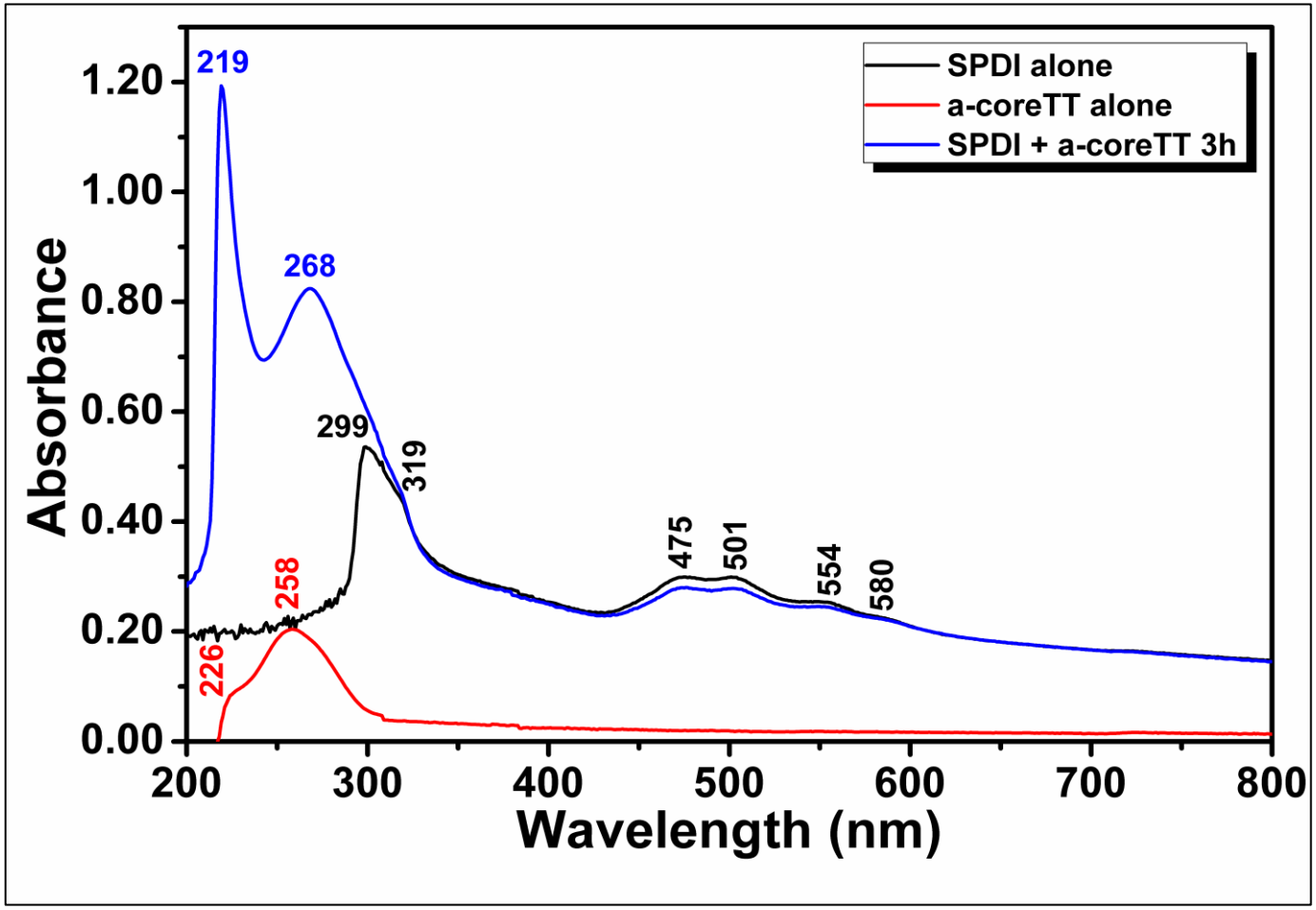

Figure 4.14: SPDI and a-coreTT, Absorption Spectrum (1M Tris-HCl Buffer pH 7.4)

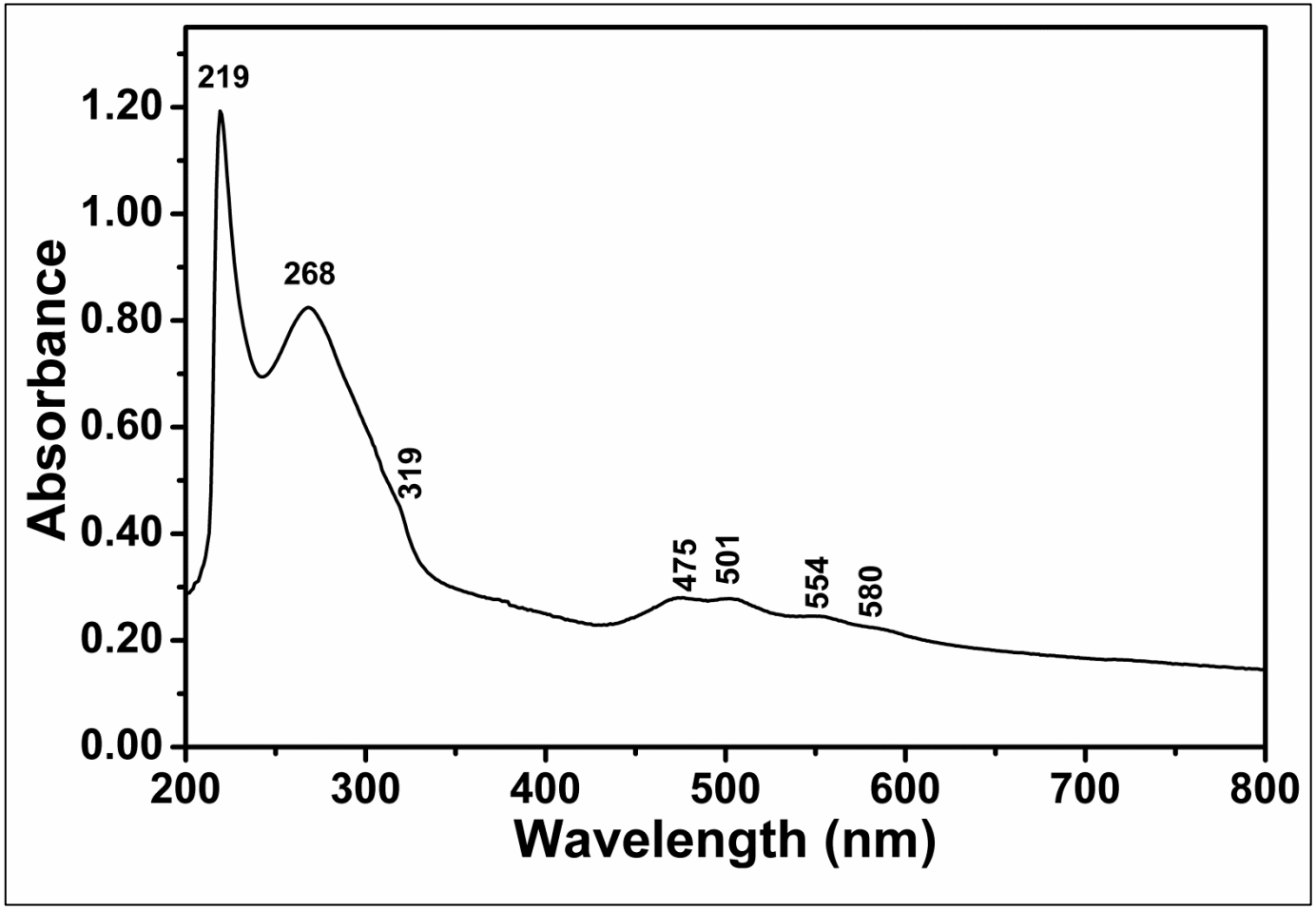

Figure 4.15: SPDI and a-coreTT, Absorption Spectrum (1M Tris-HCl Buffer pH 7.4)

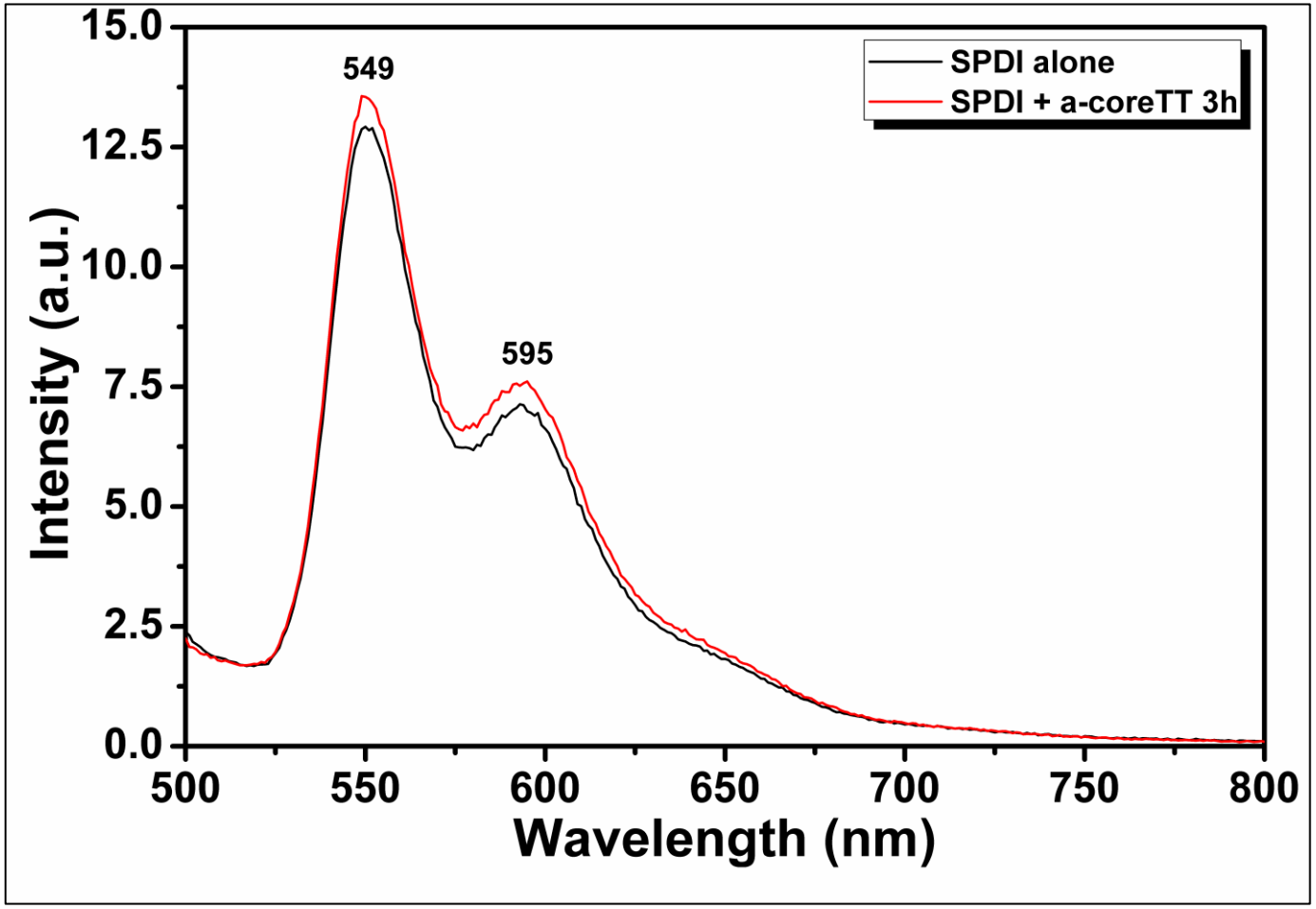

Figure 4.16: SPDI and a-coreTT, Emission Spectrum (1M Tris-HCl Buffer pH 7.4)
(λ_{exc} = 485 nm)

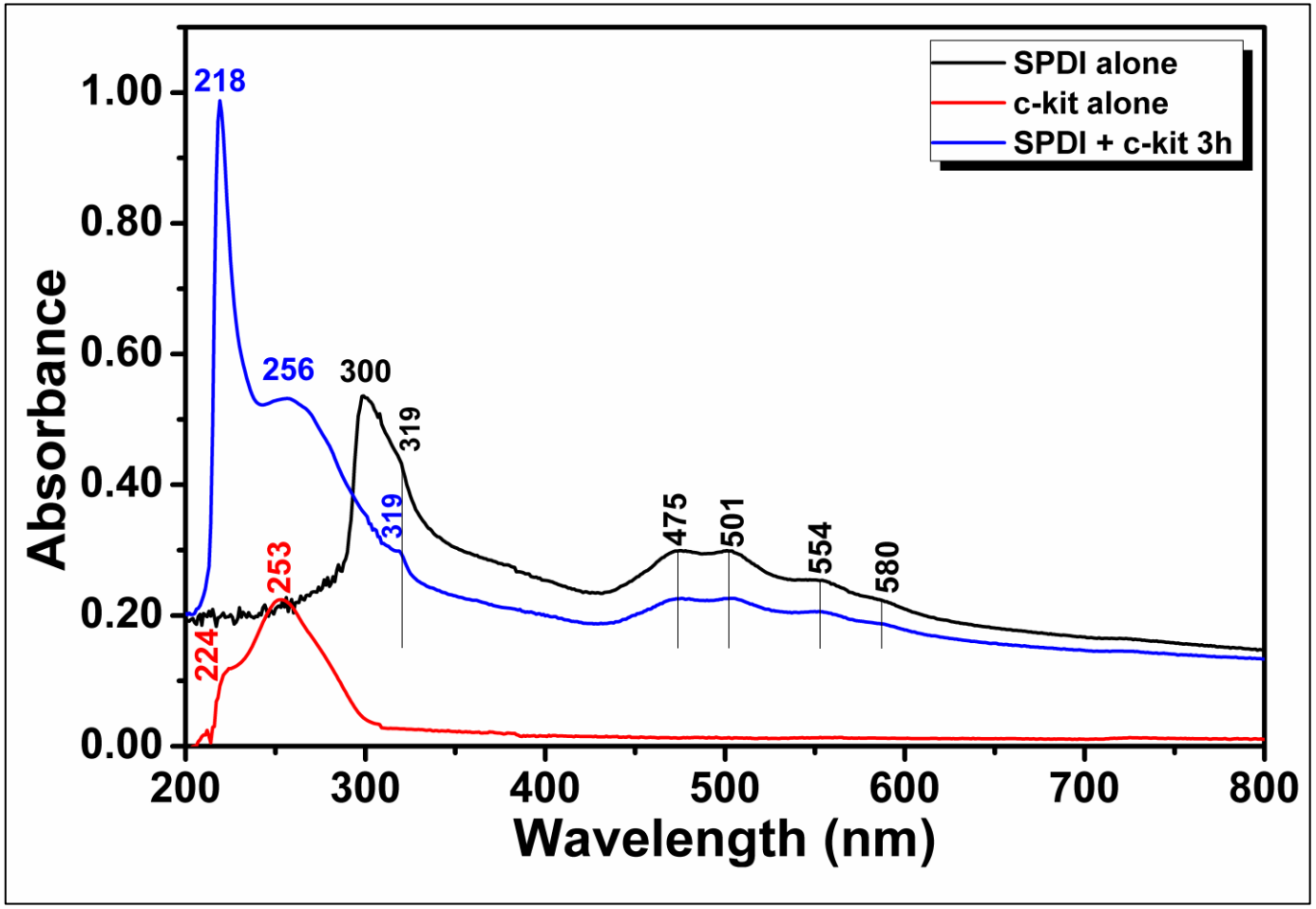

Figure 4.17: SPDI and c-kit, Absorption Spectrum (1M Tris-HCl Buffer pH 7.4)

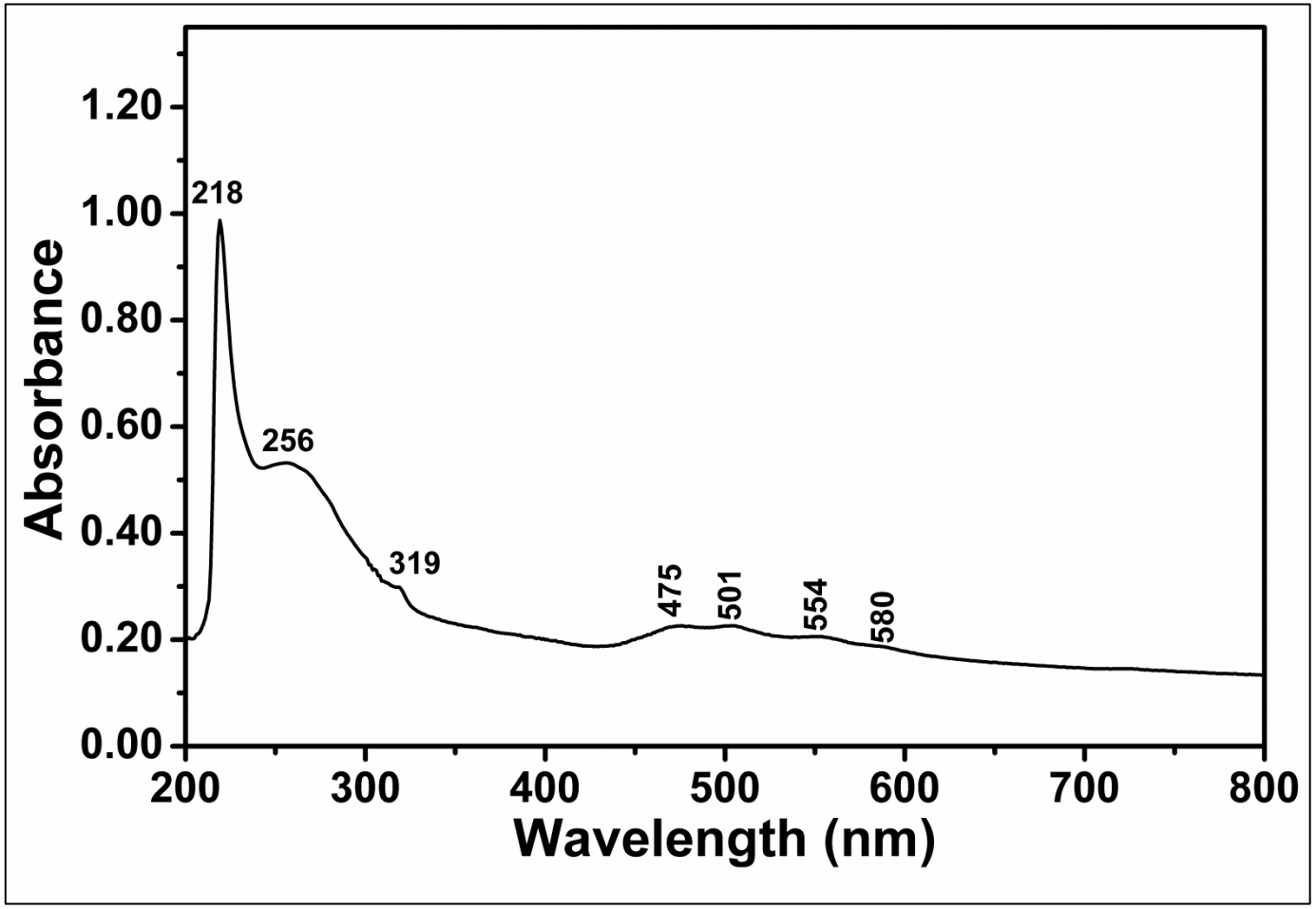

Figure 4.18: SPDI and c-kit, Absorption Spectrum (1M Tris-HCl pH 7.4)

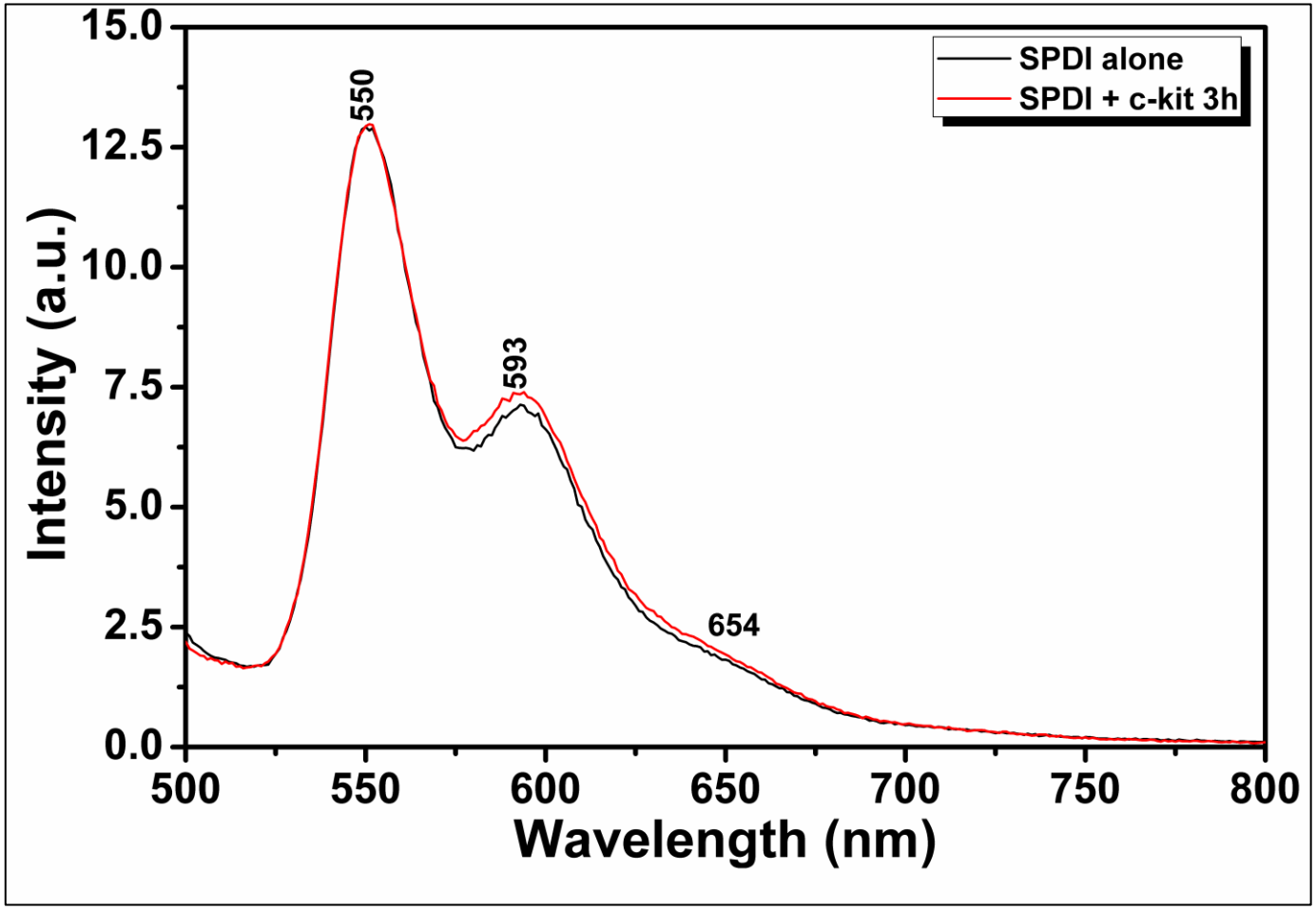

Figure 4.19: SPDI and c-kit, Emission Spectrum (1M Tris-HCl Buffer pH 7.4)
(λ_{exc} = 485 nm)

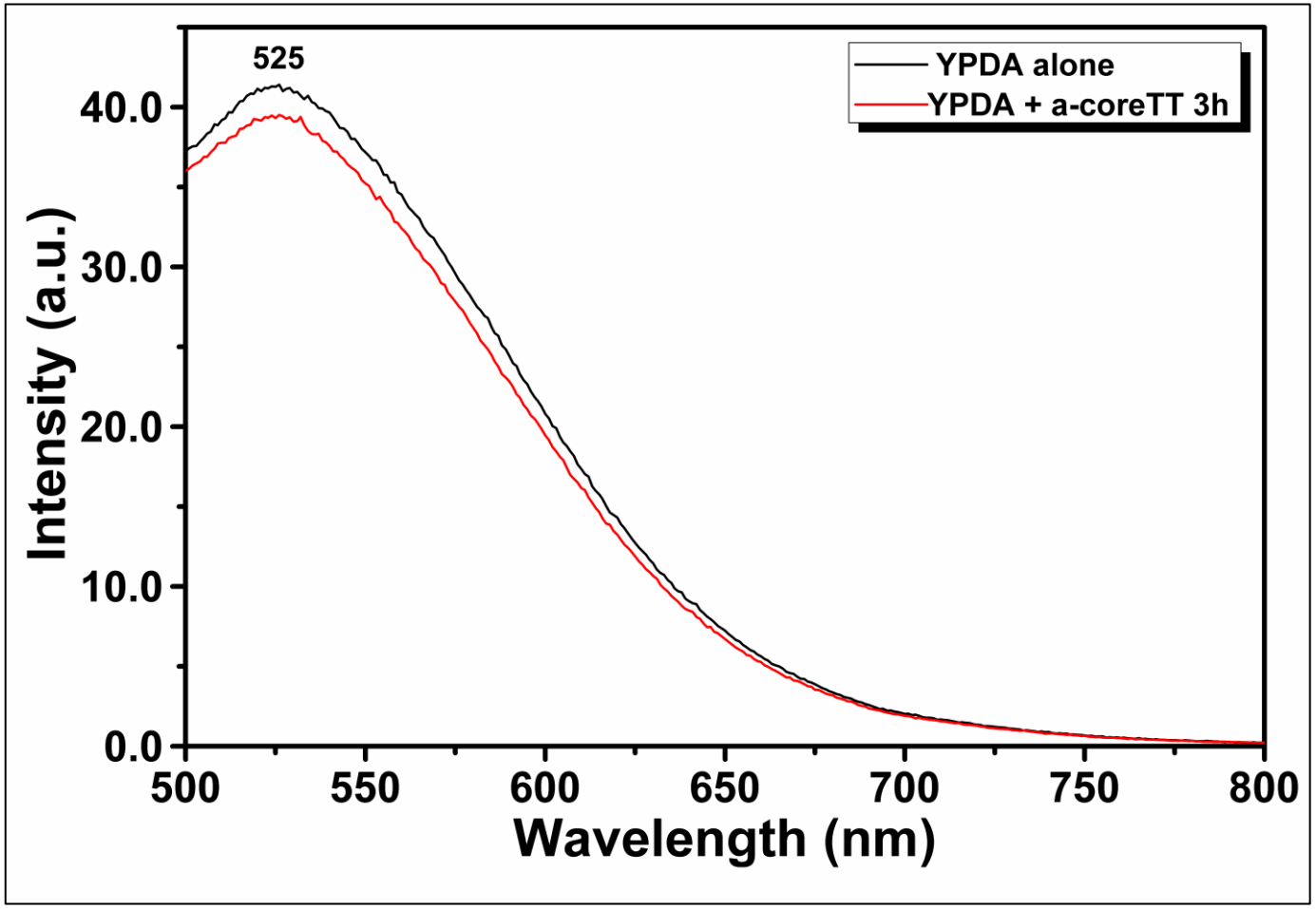

Figure 4.20: YPDA and a-coreTT, Emission Spectrum (1M Tris-HCl Buffer pH 7.4)
(λ_{exc} = 485 nm)

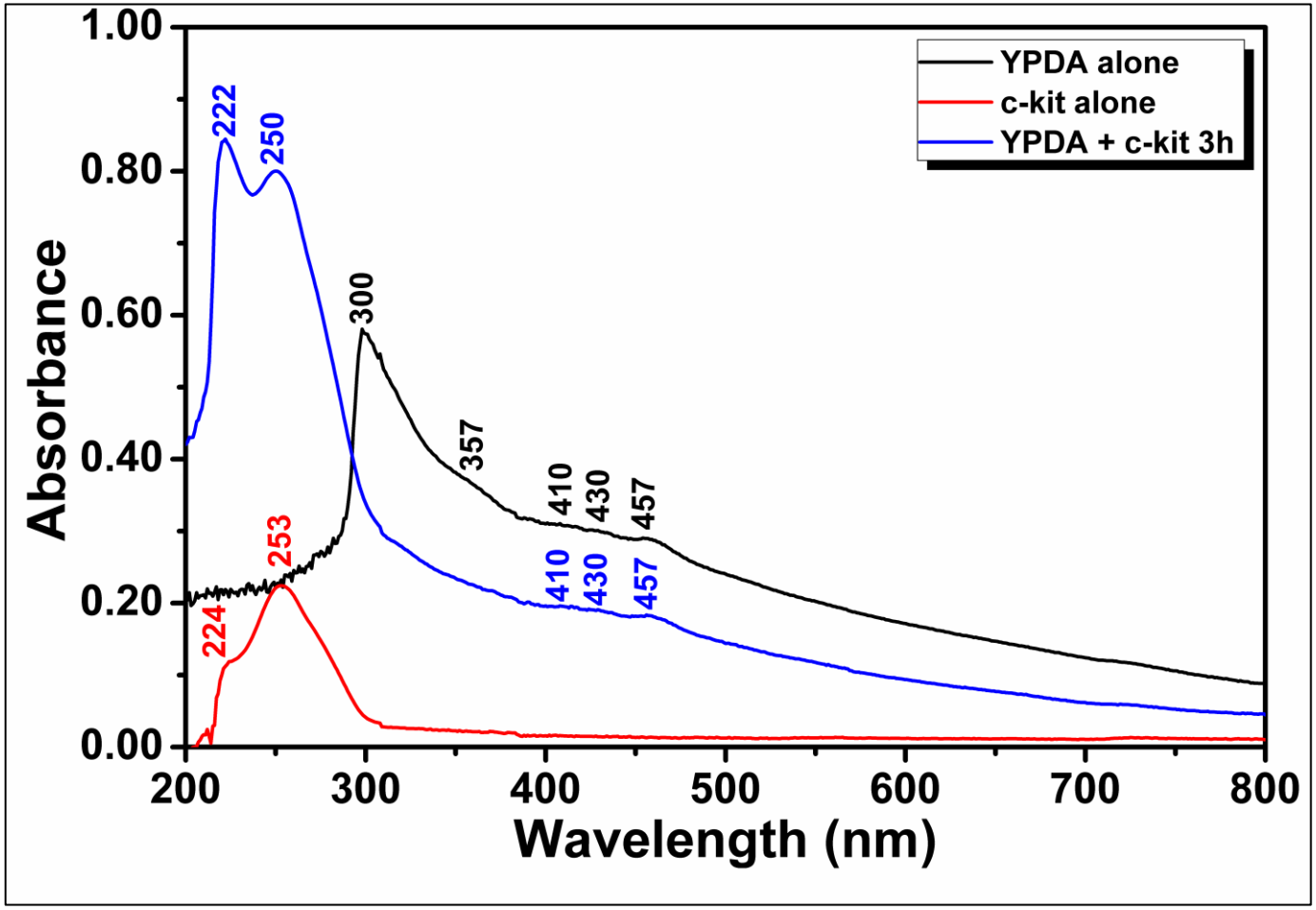

Figure 4.21: YPDA and c-kit, Absorption Spectrum (1M Tris-HCl Buffer pH 7.4)

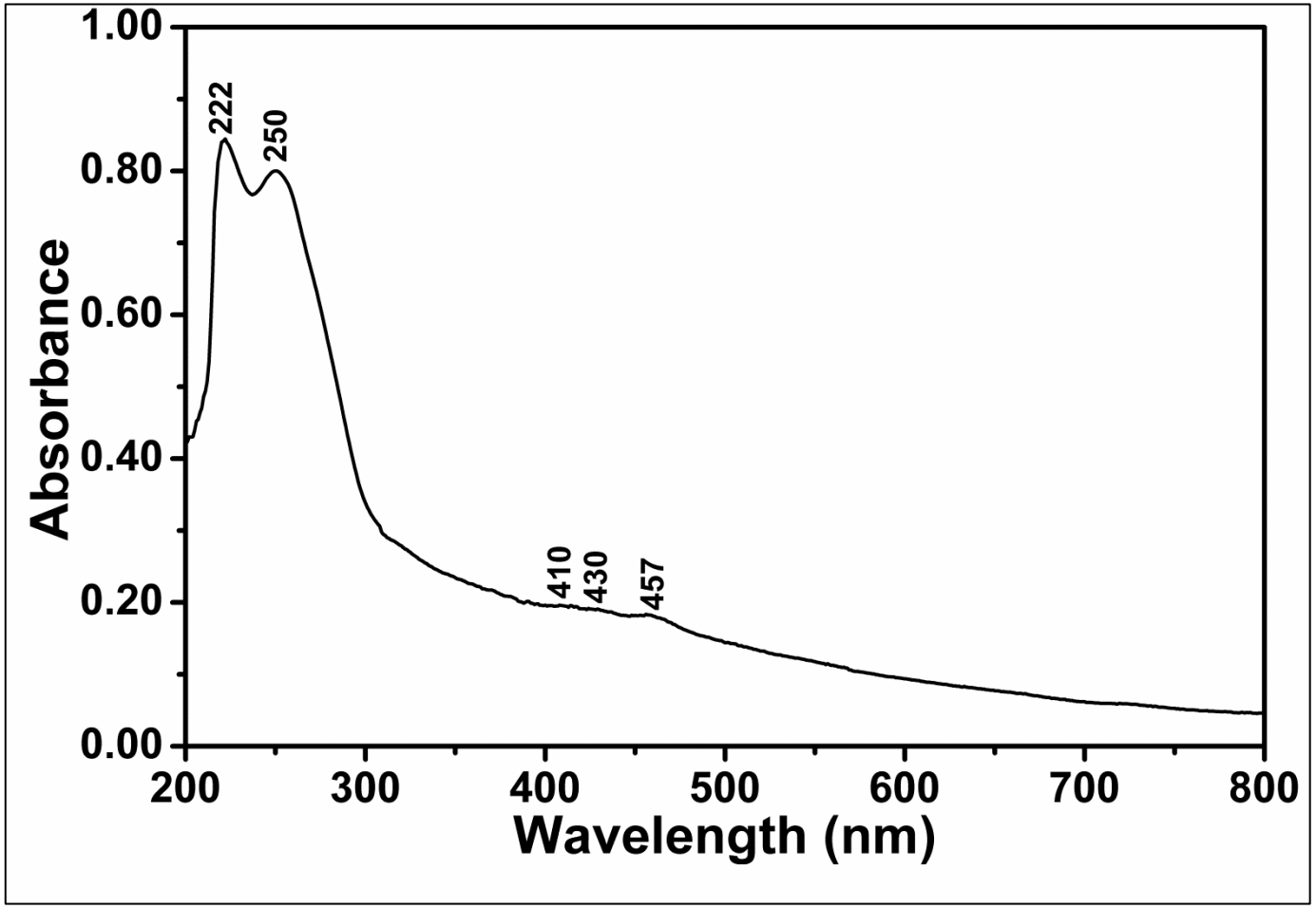

Figure 4.22: YPDA and c-kit, Absorption Spectrum (1M Tris-HCl Buffer pH 7.4)

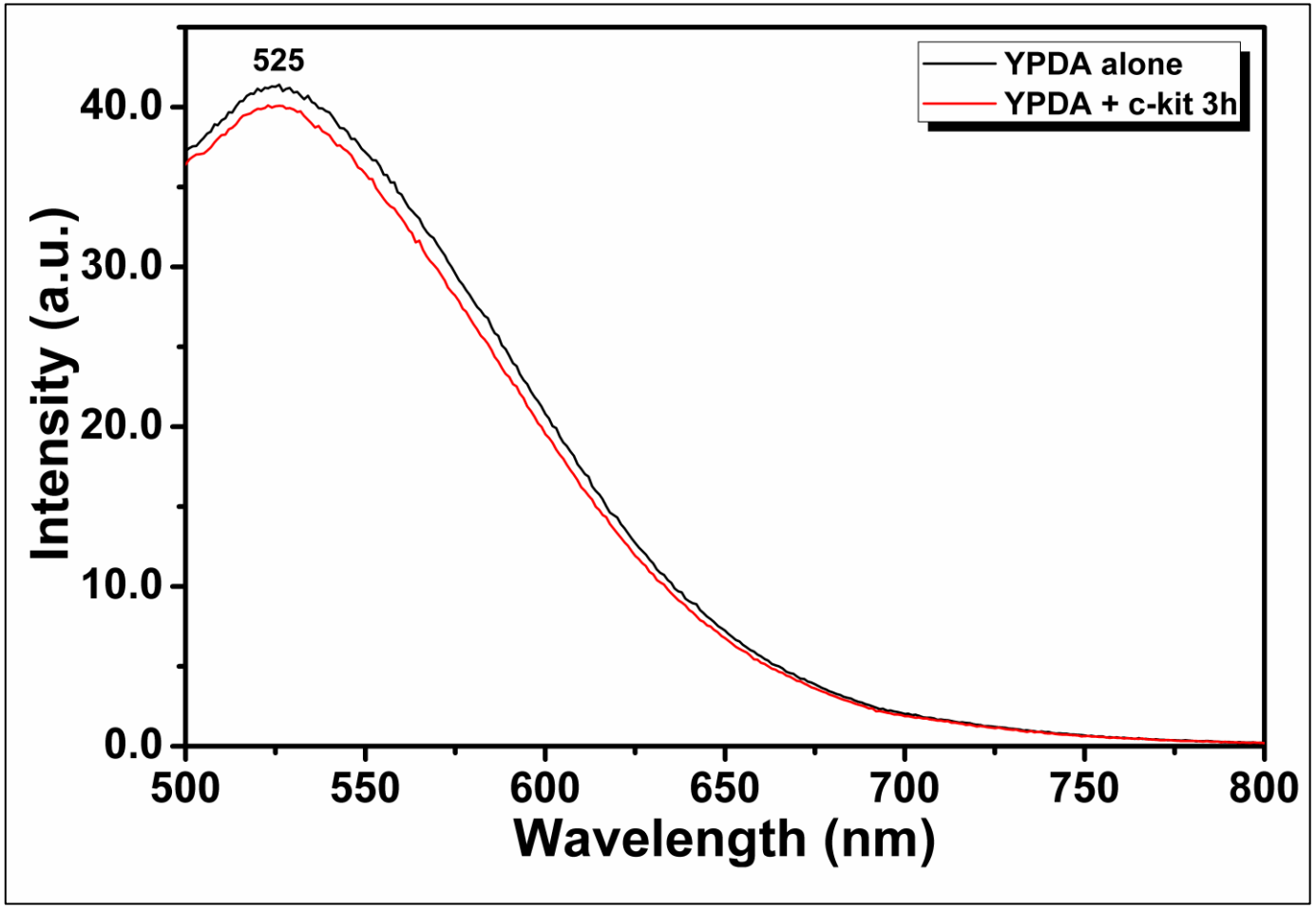

Figure 4.23: YPDI and c-kit, Emission Spectrum (1M Tris-HCl Buffer pH 7.4)
(λ_{exc} = 485 nm)

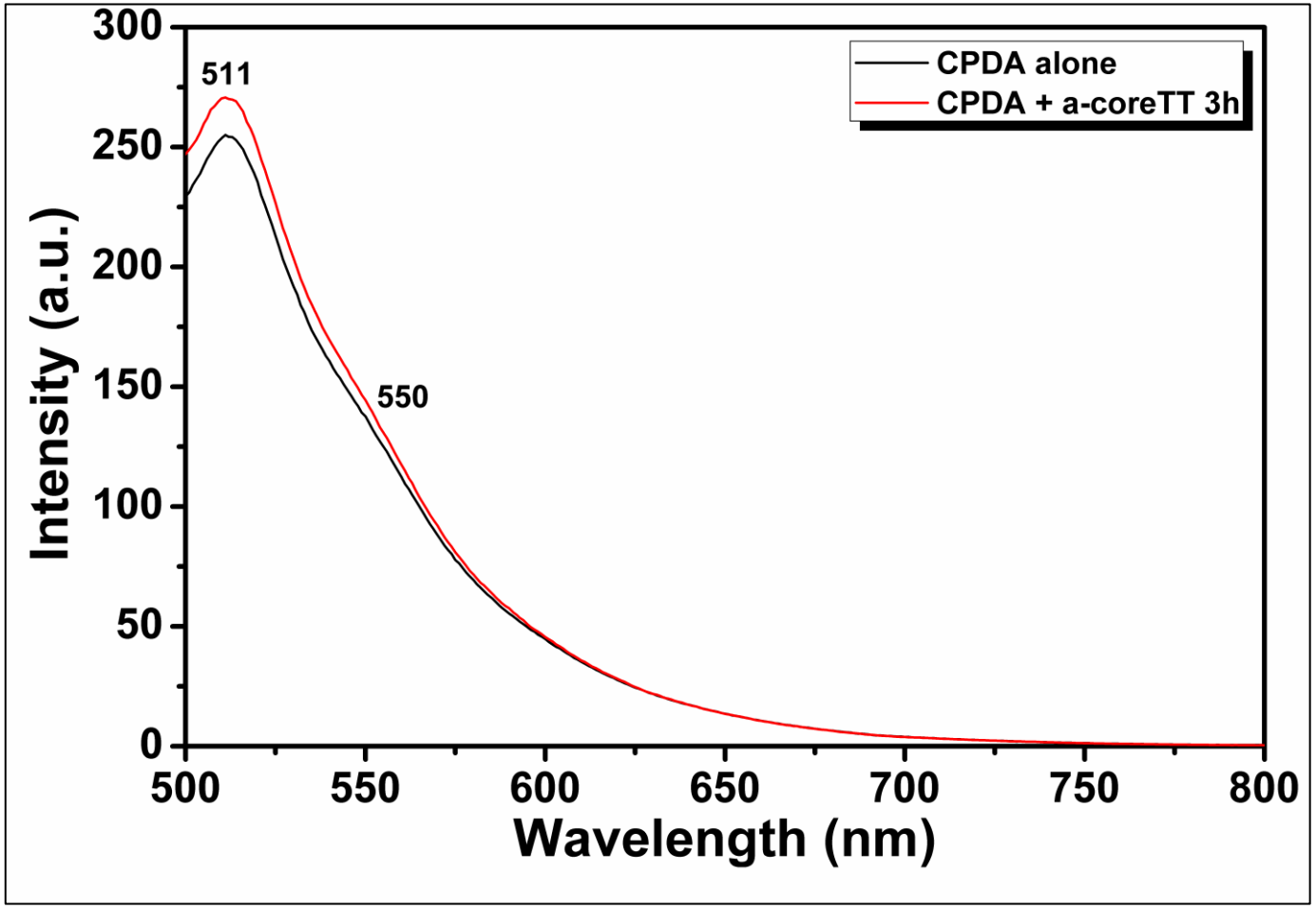

Figure 4.24: CPDA and a-coreTT, Emission Spectrum (1M Tris-HCl Buffer pH 7.4)
(λ_{exc} = 485 nm)

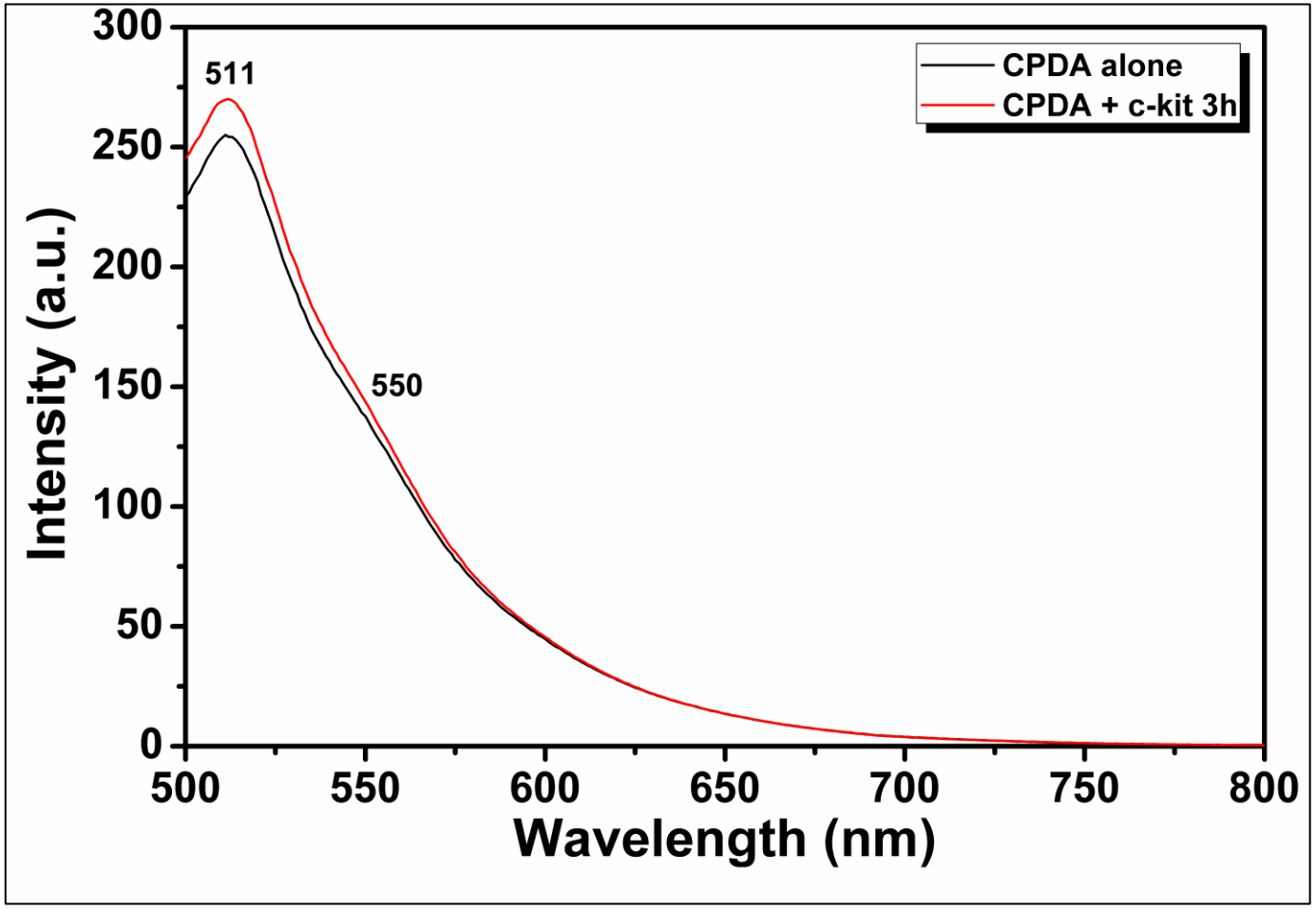

Figure 4.25: CPDA and c-kit, Emission Spectrum (1M Tris-HCl Buffer pH 7.4)
(λexc = 485 nm)

4.2 Gel Electrophoresis

All the agarose gel results are illustrated below;

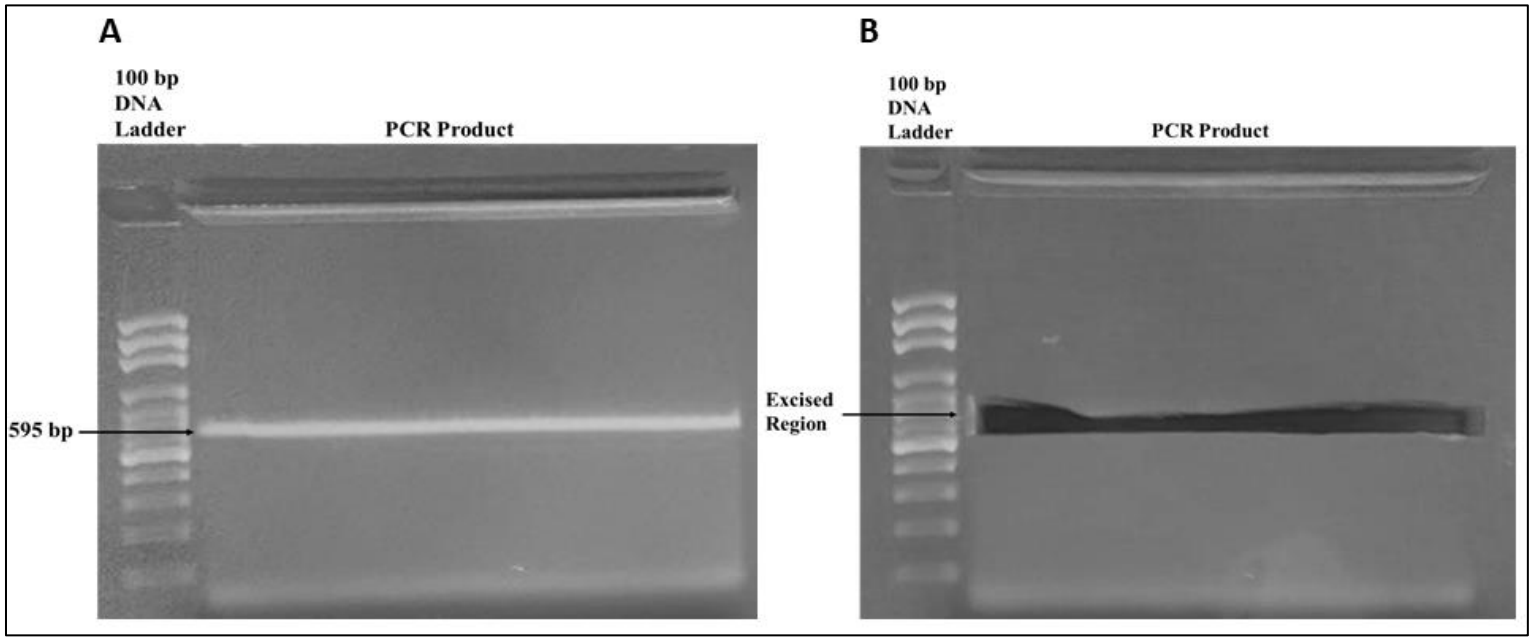

Figure 4.26: **A**) PCR Product on Gel **B**) PCR Product Excised From the Gel

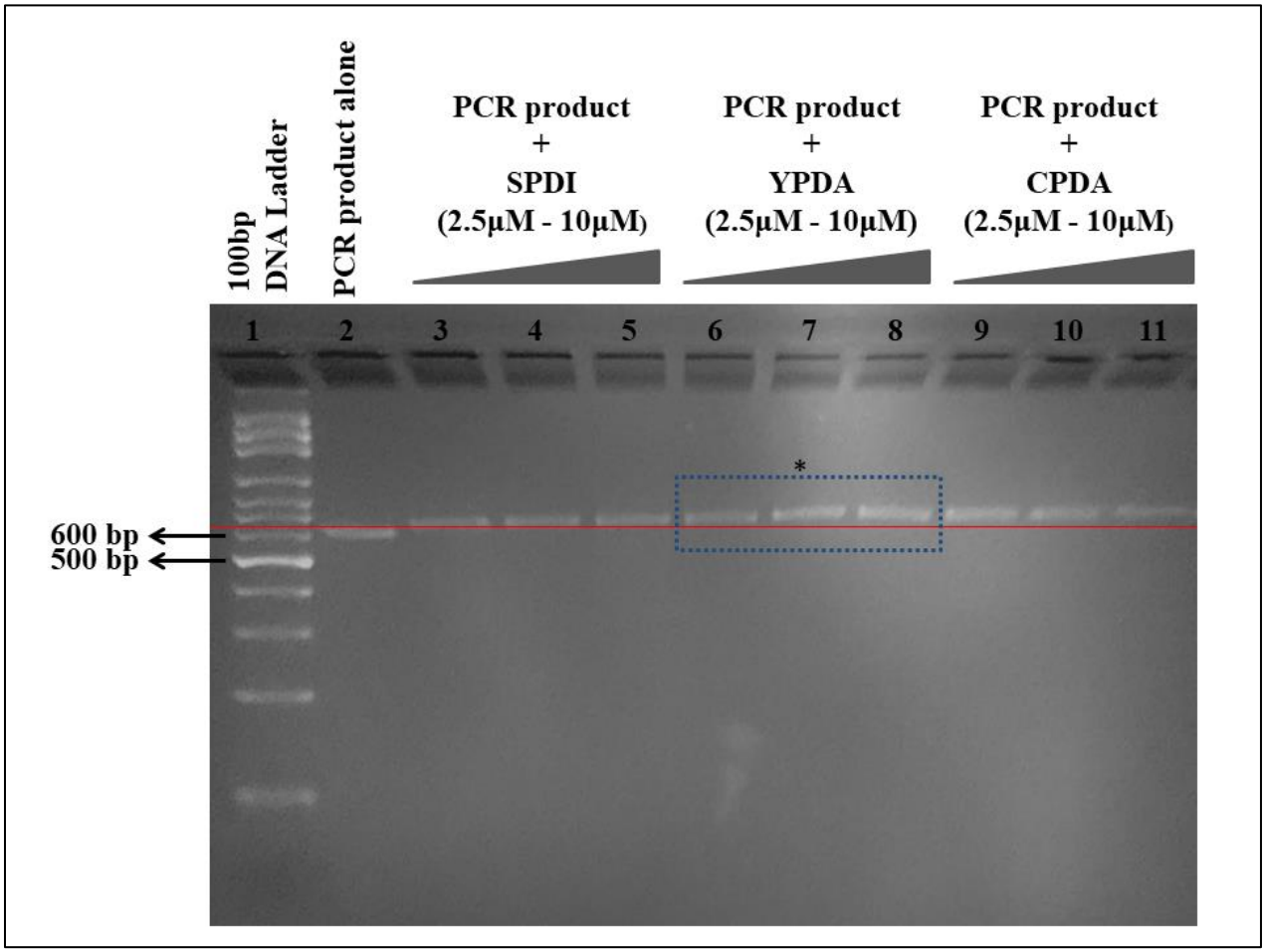

Figure 4.27: Results of the G-quadruplex Formation Assay on 4% Agarose Gel
*: YPDA concentration – dependent fragment migration
(from low to high concentration of YPDA – lanes 6 ,7, 8 in increasing YPDA concentration)

Chapter 5

RESULTS AND DISCUSSION

5.1 Absorption (UV-vis) Spectroscopy

Absorption spectra of the pure primers a-coreTT (20 μM) and c-kit (20 μM) are provided in Figure 4.4 and 4.6, respectively. Absorption spectra were recorded for all the perylene derivatives only in order to observe their aggregation behavior. A considerable decrease in absorbance was observed for SPDI over time and absorbance at 48h decreased approximately to half the absorbance at 0h as illustrated in Figure 4.8. YPDA showed a gradual slight decrease in absorbance until the 6^{th} hour but a remarkable decrease in absorbance after 24 hours. This is illustrated in Figure 4.10. CPDA on the other hand displayed a gradual slight decrease in absorbance over time and this could be observed from Figure 4.12. Overall, CPDA seems to aggregate the least, SPDI seems to aggregate the fastest and YPDA shows remarkable aggregation after 24 hours.

Absorption spectrum of the complexation of SPDI with a-coreTT is provided in Figures 4.14 and 4.15. There is an easily observable change in the peaks after the complexation takes place. This could be observed from the absorbance measurements that were taken after 3 hours of incubation at room temperature in darkness. In the region where the primer has emission, the compound has absorbance. This means that energy transfer is taking place from the primer to the compound, i.e. the energy that is emitted from the primer is being absorbed by the

compound. Remarkable splitting of the peaks related to a-coreTT could be observed with a huge increase in the absorbance of the peak at 226 nm. Similar conclusions also apply to the complexation between SPDI and c-kit but this complex additionally formed a new peak at 319 nm that just showed up as a shoulder in the absorption spectrum of the compound alone. This is illustrated in Figures 4.17 and 4.18.

The complexation of YPDA with c-kit also provided a remarkable splitting in the peaks of the primer and no new additional peaks were observed. This is illustrated in Figures 4.21 and 4.22. This also leads to a conclusion that there is an energy transfer from c-kit to YPDA. The energy that is emitted from the primer, c-kit, is being absorbed by the compound, YPDA.

The absorption spectra of the pure primers in Tris-HCl were also taken after 3 hours in order to observe whether the change in the peaks is the reason of an interaction over time between the Tris-HCl buffer and the primer itself. The absorption spectrum after 3 hours was the same as the one taken immediately after the primer was added to the buffer. This leads to a conclusion that the change in the peaks upon the complexation is the result of an interaction that is causing energy transfer from the primer to the compound.

5.2 Emission Spectroscopy

The emission spectra of the pure primers a-coreTT (20 μM) and c-kit (20 μM) are provided in Figure 4.5 and 4.7. According to the emission spectra of SPDI that is illustrated in Figure 4.9, there is a considerable increase in the two peaks with time. YPDA and CPDA also provided an increase in the peaks and most remarkably after 24 hours. Figures 4.11 and 4.13 illustrate the emission spectra of YPDA and CPDA,

respectively. This increase in emission intensity suggests energy transfer from the substituent to the perylene core, which means that energy transfer is taking place within each molecule.

The emission spectra of the complex of SPDI with a-coreTT (Figure 4.16) illustrate a slight increase in absorbance but a stable λ_{max} when compared to the pure compound alone. The emission spectra of the complex of SPDI with c-kit (Figure 4.19) illustrate an increase in the intensity of the peak at 593 nm but the peak at 550 nm did not show an increase in the intensity of emission, but rather stayed constant after 3 hours.

The interaction of YPDA with a-coreTT and c-kit provided a decrease in the intensity of emission at 525 nm for both of the interactions. The results are illustrated in Figures 4.20 and 4.23, for YPDA and a-coreTT and YPDA and c-kit, respectively.

The emission spectra of CPDA with a-coreTT and c-kit illustrate similar results with the interaction of YPDA with the two primers. Figures 4.24 and 4.25 illustrate the increase in intensity of emission for both of the interactions.

5.3 Gel Electrophoresis

The interaction of SPDI, YPDA and CPDA with the PCR amplified guanine rich region of the human beta globin gene (exon I, exon II and 60 bp of intron II after exon II) was investigated via gel electrophoresis and visualized by gel documentation and analysis system. The investigated region is illustrated in Figure 3.2. The results of the agarose gel show that bands that contain the PCR product alone migrate faster than the bands that contain the PCR product and the perylene derivative together. This is illustrated in Figure 4.27. When the band migrations were compared with the aid of a straight line as illustrated in Figure 4.27, a difference in the distance run by

the bands could be clearly observed. This difference could be attributed to the formation of a stable G-quadruplex (G4) structure as a result of the binding of the perylene derivative to the PCR product.

CPDA migrates the slowest when compared to the other two perylene derivatives SPDI and YPDA. The possible reasons might be the ionization of the side chains so that the positively charged (cationic) nitrogen ion can attract the negatively charged DNA backbone strongly. Bands with bigger size (molecular weight, M_w) migrate slower than bands with smaller size in gel electrophoresis. Therefore another possible reason might be the M_w of CPDA as it has the highest M_w when compared with the other two perylenes. Overall, CPDA possibly has a potential of higher binding affinity to this G-rich region of the human genome.

Different concentrations (two-fold dilutions from 10 μM to 2.5 μM) of the perylene derivatives were loaded into the agarose gel wells in order to observe the effect of concentration on the formation of a stable G4 structure. There was no noticeable difference between the bands with the different SPDI and CPDA concentration however the bands with YPDA and the PCR product seems to migrate slower upon increasing YPDA concentration. This suggests that YPDA induces G4 formation at a much lower concentration than the other perylene derivatives. Figure 4.27 illustrates the concentration dependent migration of the bands with YPDA and the PCR product. This region is shown with a dotted rectangle and an asterisk.

Chapter 6

CONCLUSION

In this thesis, a guanine rich region from the human beta globin gene (exon I, exon II and 60 bp of intron II after exon II) was amplified via polymerase chain reaction (PCR). This PCR product was then complexed with two perylene dianhydride derivatives and one perylene diimide derivative in order to observe whether guanine rich regions throughout the human genome could form stable G-quadruplex (G4) structures upon the presence of perylene derivatives. Additionally, a-coreTT and c-kit were used as telomeric and promoter region oligonucleotides respectively, in order to study their interaction with the perylene derivatives. The investigations were carried out with UV-vis spectroscopy, emission spectroscopy and gel electrophoresis.

An advantage of perylenes which make them interesting molecules for science is their adjustable properties according to the desired field of study. This means that perylenes with different side chains at their imide or bay positions could provide them better binding affinity to the human genome, which is our study of interest.

Spectroscopic investigations were carried out to observe if any interaction is taking place between the perylene derivatives and the primers from the human telomeres (a-coreTT) and the promoter of an oncogene (c-kit). Absorption spectroscopy illustrated an additional small peak (for SPDI and c-kit) and increase in absorbance of the pure compounds and primers upon the complexation. Emission spectroscopy provided

increase in the intensity of emission of the compounds when the complexation was carried on. Overall, spectroscopic investigations have provided results that could be attributed to energy transfer from the primers to the compounds upon the interaction. This was proven by the emission of the primers being in the same region as the absorbance of the compounds.

According to the agarose gel electrophoresis results, a difference in the migration pattern of the bands with the complex was investigated when compared to the PCR fragments alone. This suggests the formation of stable G4 structures with the help of the perylene derivatives and furthermore CPDA having the potential of higher binding affinity. Interestingly, this PCR product and perylene complexation study was performed and analyzed via the gel electrophoresis technique for the first time at our university. Here we were able to join two disciplines which are molecular biology and organic chemistry together to end up with an interesting study.

To conclude, the interaction of three perylene derivatives with a guanine rich region from the human beta globin gene and guanine rich primers from human telomeres and oncogenes was studied and was decided that further investigation should be performed to elucidate the feasibility of the perylene derivatives as future therapeutic agents.

REFERENCES

[1] Manzoor, T., Asmi, S., Niaz, S., Pandith, A. (2017). Computational studies on optoelectronic and charge transfer properties of some perylene-based donor-p-acceptor systems for dye sensitized solar cell applications. *Int. J. Quantum Chem*. 117, 1-14.

[2] Vajiravelu, S., Ramunas, L., Vidas, G., Valentas, G., Vygintasc, J., Valiyaveettil, S. (2009). Effect of substituents on the electron transport properties of bay substituted perylene diimide derivatives. *J. Mater. Chem*. 19, 4268-4275.

[3] Yin, M., Lü, B. (2017). Amphiphilic Ionic Perylenediimides: Structures, Self-Assembly Studies and Biomedical Applications. In: Kilislioğlu, A. and Karakuş, S. Molecular Self-assembly in Nanoscience and Nanotechnology. China: InTech. 27-40.

[4] Chen, H., Guan, Y., Yuan, G., Zhang, Q., Jing, N. (2014). A perylene derivative regulates HIF-1α and Stat3 signaling pathways. *Bioorg. Med. Chem*. 22, 1496-1505.

[5] Taka, A., Joonlasak, K., Huang, L., Lee, TR., Chang, S., Tuntiwechapikul, W. (2012). Down-regulation of the human VEGF gene expression by perylene monoimide derivatives. *Bioorg. Med. Chem*. Lett. 22, 518-522.

[6] Cian, A., Cristofari, G., Reichenbach, P., Lemos, E., Monchaud, D., Fichou, M., Shin-ya, K., Lacroix, L., Lingner, J., Mergny, J. (2007). Reevaluation of

telomerase inhibition by quadruplex ligands and their mechanisms of action. *Proc. N. A. S*. 104, 17347-17352.

[7] Sissi, C., Lucatello, L., Krapcho, A., Maloney, D., Boxer, M., Camarasa, M., Pezzoni, G., Mentac, E., Palumbo, M. (2007). Tri-, tetra- and heptacyclic perylene analogues as new potential antineoplastic agents based on DNA telomerase inhibition. *Bioorg. Med. Chem*. 15, 555-562.

[8] Rossetti, L., Franceschin, M., Bianco, A., Ortaggib, G., Savinoa, M. (2002). Perylene Diimides with Different Side Chains are Selective in Inducing Different G-Quadruplex DNA Structures and in Inhibiting Telomerase. *Bioorg. Med. Chem. Lett*. 12, 2527-2533.

[9] Xu, Z., Guo, K., Yu, J., Sun, H., Tang, J., Shen, J., Müllen,K., Yang, W., Yin, M. (2014). A Unique Perylene-Based DNA Intercalator: Localization in Cell Nuclei and Inhibition of Cancer Cells and Tumors. *small*. 10, 4087-4092.

[10] Todd, A., Haider, S., Parkinson, G., Neidle, S. (2007). Sequence occurrence and structural uniqueness of a G-quadruplex in the human c-kit promoter. *Nucleic Acids Research*. 35, 5799-5808.

[11] Siddiqui-Jain, A., Grand, C., Bearss, D., Hurley, L. (2002). Direct evidence for a G-quadruplex in a promoter region and its targeting with a small molecule to repress c-MYC transcription. *Proc. N. A. S*. 99, 11593-11598.

[12] Bejugam, M., Sewitz, S., Shirude, P., Rodriguez, R., Shahid, R., Balasubramanian, S. (2007). Trisubstituted Isoalloxazines as a New Class of G-Quadruplex Binding Ligands: Small Molecule Regulation of c-kit Oncogene Expression. *J. Am. Chem. Soc*. 129, 12926-12927.

[13] Chu, B., Yuan, G., Zhou, J., Ou, Y., Zhu, P. (2008). A New Telomerase Inhibitor and Apoptosis-Inducing Agent in Leukemia: Perylene Derivative G-Quadruplex Ligand Tel03. *Drug Dev. Res*. 69, 235-241.

[14] Taka, A., Huang, L., Wongnoppavich, A., Chang, S., Lee, T., Tuntiwechapikul, W. (2013). Telomere shortening and cell senescence induced by perylene derivatives in A549 human lung cancer cells. *Bioorg. Med. Chem. Lett*. 21, 883-890.

[15] Rossetti, L., Franceschin, M., Schirripa, S., Bianco, A., Ortaggi, G., Savino, M. (2005). Selective interactions of perylene derivatives having different side chains with inter- and intramolecular G-quadruplex DNA structures. A correlation with telomerase inhibition. *Bioorg. Med. Chem. Lett*. 15, 413-420.

[16] Kerwin, S., Chen, G., Kern, J., Thomas, P. (2002). Perylene Diimide G-Quadruplex DNA Binding Selectivity is Mediated by Ligand Aggregation. *Bioorg. Med. Chem. Lett*. 12, 447-450.

[17] Mullis, K., Faloona, F., Scharf, S., Saiki, R., Horn, G., Erlich, H. (1986). Specific Enzymatic Amplification of DNA In Vitro: The Polymerase Chain Reaction. *Cold Spring Harb Symp Quant Biol*. 51, 263-273.

[18] Tuzmen, S., Schechter, AN., (2001). Genetic diseases of hemoglobin: diagnostic methods for elucidating β-thalassemia mutations. *Blood Reviews*. 15 (1), 19-29.

[19] Islam, M., Fujii, S., Sato, S., Okauchi, T., 1 Takenaka, S. (2015). A Selective G-Quadruplex DNA-Stabilizing Ligand Based on a Cyclic Naphthalene Diimide Derivative. *Molecules*. 20, 10963-10979.

[20] Watson. JD., Crick, FH. (1953). Molecular structure of nucleic acids; a structure for deoxyribose nucleic acid. *Am J Psychiatry*. 171, 737-738.

[21] Crick, FHC., Watson, JD. (1954). The complementary structure of deoxyribonucleic acid. *Royal Society*. 223, 80-96.

[22] Bailey, R. (2017). Learn About Nucleic Acids. Available: https://www.thoughtco.com/nucleic-acids-373552. Last accessed 10th Jul 2018.

[23] Pradhan, AB., Haque, L., Bhuiya, S., Das, S. . (2015). Exploring the mode of binding of the bioflavonoid kaempferol with B and protonated forms of DNA using spectroscopic and molecular docking studies. *RSC Adv*. 10219-10230.

[24] Gellert, I., Lipsett, MN., Davies, DR. (1962). Helix Formation by Guanylic Acid. Proc. N. A. S. 48, 2013-2018.

[25] Bochman, M., Paeschke, K., Zakian, V. (2012). DNA secondary structures: stability and function of Gquadruplex structures. *Nat. Rev. Genet*. 13, 770-780.

[26] Edwards, DN., Machwe, A., Wang1, Z., Orren, DK. (2014). Intramolecular Telomeric G-Quadruplexes Dramatically Inhibit DNA Synthesis by Replicative and Translesion Polymerases, Revealing their Potential to Lead to Genetic Change. *Plos One*. 9, e80664- e80664.

[27] Víglaský, V., Bauer, L., Tlucková, K. (2010). Structural Features of Intra- and Intermolecular G-Quadruplexes Derived from Telomeric Repeats. *Biochemistry*. 49, 2110-2120.

[28] Howell, RM., Woodford, KJ., Weitzmann, MN., Usdin, K.. (1996). The Chicken b-Globin Gene Promoter Forms a Novel "Cinched" Tetrahelical Structure. *J. Biol. Chem*. 271, 5208-5214.

[29] Salgado, G., Cazenave, C., Kerkourab, A., Mergny, J. (2015). G-quadruplex DNA and ligand interaction in living cells using NMR spectroscopy. *Chem. Sci*. 6, 3314-3320.

[30] Meyne, J., Ratliff, RL., AND Moyzis, RK. (1989). Conservation of the human telomere sequence (TTAGGG)n among vertebrates. *Proc. Natl. Acad. Sci*. 86, 7049-7053.

[31] Griffith, JD. Comeau, L., Rosenfield, S., Stansel, RM., Bianchi, A., Moss, H., de Lange, T. (1999). Mammalian Telomeres End in a Large Duplex Loop. *Cell*. 97, 503-514.

[32] Olovnikov, AM. (1996). Telomeres, Telomerase, and Aging: Origin of the Theory. *Experimental Gerontology*. 31, 443-448.

[33] Deng, Y., Chan, S., Chang,S. (2008). Telomere dysfunction and Tumor Suppression-the Senescence Connection. *Nat Rev Cancer*. 8, 450-458.

[34] Cong,, YS., Wright, WE., Shay, JW. (2002). Human Telomerase and Its Regulation. *Microbiology and Molecular Biology Reviews*. 66, 407-425

[35] Mergny, JL., Helene, C. (1998). G-quadruplex DNA: A target for drug design. *Nature Medicine*. 4, 1366-1367.

[36] Vorlíčková, M., Chládková, J., Kejnovská, I., Fialová, M., Kypr, J. (2005). Guanine tetraplex topology of human telomere DNA is governed by the number of (TTAGGG) repeats. *Nucleic Acids Research*. 33, 5851-5860.

[37] Huppert, JL., Balasubramanian, S. (2005). Prevalence of quadruplexes in the human genome. *Nucleic Acids Research*. 33, 2908-2916.

[38] Balasubramanian, S., Hurley, LH., Neidle, S. (2011). Targeting G-quadruplexes in gene promoters: a novel anticancer strategy?. *Nat Rev Drug Discov*. 10, 261-275.

[39] Rankin, S., Reszka, AP., Huppert, J., Zloh, M., Parkinson, GN., Todd, AK., Ladame, S., Balasubramanian, S., Neidle, S. (2005). Putative DNA Quadruplex

*Formation within the Human c-kit Oncogene. J. Am. Chem. Soc. 127, 10584-*10589.

[40] Phan, AT., Kuryavyi, V., Gaw, HY., Patel, DJ. (2005). Small-molecule interaction with a five-guanine-tract Gquadruplex structure from the human MYC promoter. *Nat Chem Biol*. 1,167-173.

[41] Sun, D., Guo, K., Rusche1, JJ., Hurley, LH. (2005). Facilitation of a structural transition in the polypurine/polypyrimidine tract within the proximal promoter region of the human VEGF gene by the presence of potassium and G-quadruplex-interactive agents. *Nucleic Acids Res*. 33, 6070-6080.

[42] Kim, M., Gleason-Guzman, M., Izbicka, E., Nishioka, D., and Hurley, L. (2003). The Different Biological Effects of Telomestatin and TMPyP4 Can Be Attributed to Their Selectivity for Interaction with Intramolecular or Intermolecular G-Quadruplex Structures. *Cancer Research*. 63, 3247-3256.

[43] Woodford, KJ., Howell, RM., Usdi, K.. (1994). A Novel K+-dependent DNA Synthesis Arrest Site in a Commonly Occurring Sequence Motif in Eukaryotes. *J. Biol. Chem*. 269 (43), 27029-27035.

[44] Kim, CG., Epner, EM., Forrester, WC., Groudine, M. (1992). Inactivation of the human beta-globin gene by targeted insertion into the beta-globin locus control region. *Genes & Dev*. 6, 928-938.

[45] Samudrala, R., Zhang, X., Wadkins, RM., Mattern, DL. (2007). Synthesis of a non-cationic, water-soluble perylenetetracarboxylic diimide and its interactions with G-quadruplex-forming DNA. *Bioorg. Med. Chem*. 15, 186-193.

[46] Street, STG., Chin, DN., Hollingworth, GJ., Berry, M., Morales, JC., Galan, MC. (2017). Divalent Naphthalene Diimide Ligands Display High Selectivity for the Human Telomeric G-quadruplex in K+ Buffer. *Chem. Eur. J*. 23, 6953-6958.

[47] Zhang, LN., Zhang, R., Cui, YX., Liu, KK., Kong, DM., Li, XZ., Zhu, LN. (2017). Highly specific G-quadruplex recognition covering physiological pH range by a new water-soluble cationic porphyrin with low self-aggregation tendency. *Dyes and Pigments*. 145, 404-417.

[48] Micheli1, E., Altieri, A., Cianni, L., Cingolani, C., Iachettini, S., Bianco, A., Leonetti, C., Cacchione, S., Biroccio, A., Franceschin, M., Rizzo, A. (2016). Perylene and coronene derivatives binding to G-rich promoter oncogene sequences efficiently reduce their expression in cancer cells. *Biochimie*. 125, 223-231.

[49] Maleki, P., Ma, Y., Iida, K., Nagasawa, K., Balci, H. (2017). A single molecule study of a fluorescently labeled telomestatin derivative and G-quadruplex interactions. *Nucleic Acids Research*. 45, 288-295.

[50] Chen, K., Chang, C. (2014). Highly Soluble Monoamino-Substituted Perylene Tetracarboxylic Dianhydrides: Synthesis, Optical and Electrochemical Properties. *International Journal of Molecular Sciences*. 15, 22642-22660.

[51] Pasaogullari, N., Icil, H., Demuth, M., (2006). Symmetrical and unsymmetrical perylene diimides: Their synthesis, photophysical and electrochemical properties. *Dyes and Pigments*. 69, 118-127.

[52] Avlasevich, Y., Li, C., Müllen, K. (2010). Synthesis and applications of core-enlarged perylene dyes. *Journal of Materials Chemistry*. 20, 3814-3826.

[53] Rao, L., Dworkin, J., Nell, W., Bierbach, U. (2011). Interactions of a Platinum-Modified Perylene Derivative with the Human Telomeric G-Quadruplex. *The Journal of Physical Chemistry*. 115, 13701-13712.

[54] Monchaud, D., Allain, C., Bertrand, H., Smargiasso, N., Rosu, F., Gabelica, V., De Cian, A., Mergny, -JL., Teulade-Fichou, M.-P. (2008). Ligands playing musical chairs with G-quadruplex DNA: A rapid and simple displacement assay for identifying selective G-quadruplex binders. *Biochimie*. 90, 1207-1223.

[55] Kaushik, M., Kaushik, S., Bansal, A., Saxena, S., Kukreti, S. (2011). Structure-Specific Ligand Recognition of Multistranded DNA Structures. *Current Molecular Medicine*. 11, 744-769.

[56] Wei, C., Jia, G., Zhou, J., Hana, G., Li, C. (2009). Evidence for the binding mode of porphyrins to G-quadruplex DNA. *Phys. Chem. Chem. Phys*. 11, 4025-4032.

[57] Hou, JQ., Chen, SB., Tan, JH., Luo, HB., Li, D., Gu, LQ., Huang, ZS. (2012). New insights from molecular dynamic simulation studies of the multiple binding modes of a ligand with G-quadruplex DNA. *J Comput Aided Mol Des*. 26, 1355-1368.

[58] Ou, T., Lu, Y., Tan, J., Huang, Z., Wong, K., Gu, L. (2008). G-Quadruplexes: Targets in Anticancer Drug Design. *ChemMedChem*. 3, 690-713.

[59] Chen, BJ., Wu, YL., Tanaka, Y., Zhang, W. (2014). Small Molecules Targeting c-Myc Oncogene: Promising Anti-Cancer Therapeutics. *Int. J. Biol. Sci*. 10, 1084-1096.

APPENDIX

Doğu Akdeniz Üniversitesi
"Uluslararası Kariyer İçin"

Eastern Mediterranean University
"For Your International Career"

P.K.: 99628 Gazimağusa, KUZEY KIBRIS / *Famagusta, North Cyprus, via Mersin-10 TURKEY*
Tel: (+90) 392 630 1995
Faks/*Fax*: (+90) 392 630 2919
bayek@emu.edu.tr

Etik Kurulu / *Ethics Committee*

Sayı: ETK00-2018-0201 13.07.2018
Konu: Etik Kurulu'na Başvurunuz Hk.

Arwa Abou Rajab

Fen ve Edebiyat Fakültesi
Yüksek Lisans Öğrencisi

Doğu Akdeniz Üniversitesi Bilimsel Araştırma ve Yayın Etiği Kurulu'nun ***21.05.2018*** tarih ve ***2018/59-16*** sayılı kararı doğrultusunda, ***"Yeni Perilen Dianhidrid ve Diimide Setlerinin İnsan DNA'sındaki G-quadruplex Yapıları ile Etkileşimi"*** adlı çalışmanızı, Prof. Dr. Huriye İcil ve Doç. Dr. Şükrü Tüzmen'in danışmanlığında araştırmanız, Bilimsel ve Araştırma Etiği açısından uygun bulunmuştur.

Bilginize rica ederim.

Yrd. Doç. Dr. Mümtaz Güran (a)
Etik Kurulu Başkan Yardımcısı

ŞT/ba.